

OPEN ACCESS

EDITED BY

Xu Han,
Shanghai Jiao Tong University, China

REVIEWED BY

Jalil Rasgado Toledo,
National Autonomous University of
Mexico, Mexico
Wentao Hu,
Shanghai Jiao Tong University, China

*CORRESPONDENCE

Shu Wang

✉ tony20120113@163.com

Wen-Hui Li

✉ ycsylwh@gmail.com

Si-Yu Gu

✉ gsy9610@163.com

[†]These authors have contributed equally
to this work

RECEIVED 07 December 2025

REVISED 02 March 2026

ACCEPTED 13 March 2026

PUBLISHED 27 March 2026

CITATION

Xu H, Liu X-Y, Yang H-C, Pan P-L, Gu
S-Y, Li W-H and Wang S (2026) Network
localization of gray matter alterations in
chronic smokers using the normative
functional connectome.
Front. Public Health 14:1762620.
doi: 10.3389/fpubh.2026.1762620

COPYRIGHT

© 2026 Xu, Liu, Yang, Pan, Gu, Li and
Wang. This is an open-access article
distributed under the terms of the
[Creative Commons Attribution License](#)
(CC BY). The use, distribution or
reproduction in other forums is
permitted, provided the original
author(s) and the copyright owner(s) are
credited and that the original publication
in this journal is cited, in accordance
with accepted academic practice. No
use, distribution or reproduction is
permitted which does not comply with
these terms.

Network localization of gray matter alterations in chronic smokers using the normative functional connectome

Han Xu^{1†}, Xiao-Yi Liu^{1†}, Hu-Cheng Yang^{2†}, Ping-Lei Pan³,
Si-Yu Gu^{1*}, Wen-Hui Li^{1,4*} and Shu Wang^{1*}

¹Department of Radiology, Affiliated Hospital 6 of Nantong University, Yancheng Third People's Hospital, Yancheng, China, ²Binhai Maternal and Child Health Hospital, Yancheng, China, ³Department of Neurology, Affiliated Hospital 6 of Nantong University, Yancheng Third People's Hospital, Yancheng, China, ⁴Yancheng Maternal and Child Health Care Hospital, Yancheng, China

Background: Chronic smoking has well-documented impacts on brain structure. Voxel-based morphometry (VBM) investigations have revealed diverse regional gray matter (GM) changes in chronic smokers, hindering a unified understanding of smoking-induced neuropathology. To reconcile these findings, this study aimed to identify common intrinsic functional networks underlying these structural alterations using a functional connectivity network mapping (FCNM) approach. We further explored potential exposure-dependent variations to characterize how brain network architecture relates to cumulative smoking dose.

Methods: We utilized coordinate-based FCNM to quantitatively integrate heterogeneous findings from previous VBM studies. We systematically reviewed VBM studies reporting GM differences between chronic smokers and non-smokers. We identified peak coordinates from 27 studies, encompassing 36 contrasts with 1,336 smokers and 1803 non-smokers. Resting-state fMRI from 1,093 healthy participants (Human Connectome Project) were utilized to create individual functional connectivity maps based on seed coordinates. Maps were combined to identify a shared alteration network and evaluated for spatial overlap with established canonical brain networks. Sensitivity analysis were conducted with different seed radii. Crucially, subgroup analysis stratified studies into higher-exposure and lower-exposure groups to investigate exposure-dependent mechanisms.

Results: Functional connectivity network mapping identified a widespread network linked to smoking-induced GM changes. Key nodes included the supramarginal gyrus, insula, anterior cingulate cortex, caudate nucleus, putamen, and superior temporal gyrus. Spatial overlap analysis revealed predominant involvement of the posterior Salience Network (51.59%), anterior Salience Network (32.15%), basal ganglia network (31.52%), and auditory network (24.19%). Sensitivity analysis confirmed the robustness of these findings. Subgroup analysis revealed exposure-dependent patterns: while the Salience and basal ganglia networks were consistently affected in both groups, the auditory network and ventral Default Mode Network showed markedly greater involvement in the higher-exposure group, largely spared in the lower-exposure group.

Conclusion: This FCNM approach identified consistent brain networks, predominantly the Salience, basal ganglia, and auditory networks, associated with chronic smoking-related GM alterations. These findings offer network-level insight into the structural effects of smoking, helping to resolve discrepancies and potentially guiding tailored interventions. Furthermore, the findings suggest a progressive neuropathological expansion, characterized by the concurrent recruitment

of sensory (auditory) and high-order cognitive systems (ventral Default Mode Network) with cumulative smoking exposure.

KEYWORDS

basal ganglia, gray matter, network localization, Salience Network, smoking

1 Introduction

Tobacco use remains a major global public health threat, accounting for over 8 million deaths annually (1). Smoking is widely recognized for increasing the risk of cancer, respiratory diseases and cardiovascular diseases; Moreover, in addition to its adverse effects on oral, reproductive, and musculoskeletal health, smoking also causes profound damage to the nervous system (2–5). Nicotine, the primary addictive substance in cigarettes, binds to nicotinic acetylcholine receptors within key reward circuits, such as the ventral tegmental area and nucleus accumbens (6–10). This binding triggers the release of dopamine, generating a sense of pleasure and reinforcing the cycle of addiction (11). However, the regulatory effects of nicotine on dopamine in the brain are not limited to the reward circuit; nicotine may also influence other brain regions associated with mood, memory, and cognitive functions (11, 12). Other toxic compounds in cigarettes, such as carbon monoxide and free radicals, cause persistent neurological damage (e.g., cognitive decline) through mechanisms including oxidative stress, inflammation, vascular damage, and blood–brain barrier disruption (13, 14). Crucially, recent evidence links VBM-detected gray matter volume (GMV) changes directly to underlying cellular metrics, such as variations in cell density and nuclear volume (15). This suggests that smoking-induced oxidative and inflammatory burdens likely precipitate microscopic cellular alterations that manifest as macroscopic GM anomalies (16, 17). Although significant progress has been made in understanding the effects of smoking on the brain, the pathophysiology of brain changes in chronic smokers remains incompletely elucidated (18).

Over the past two decades, voxel-based morphometry (VBM) has been extensively used to examine gray matter (GM) volume alterations among chronic smokers (19–30). Compared with the manual delineation of regions of interest (ROI) for measuring brain structure volumes, VBM offers a hypothesis-free, time-efficient approach to quantifying whole-brain structural differences *in vivo* on a voxel-by-voxel basis (31). Taking advantage of this approach, numerous studies have found that chronic smokers exhibit reduced GM volume in regions such as the anterior cingulate cortex (ACC), thalamus, and cerebellum (19–24, 26, 28, 29). However, findings regarding GM volume changes in areas such as putamen, caudate nucleus and orbitofrontal cortex remain inconsistent (19–23, 26, 30, 32). Although this heterogeneity is often attributed to methodological variations, such as sample size, clinical characteristics, and analytical strategies (24, 33–37), divergent results persist even among well-controlled studies. In an attempt to synthesize these divergent VBM results, coordinate-based meta-analysis (CBMA) have been utilized to identify regions of spatial convergence, revealing consistent alterations in several regions, including the superior frontal gyrus, right lingual gyrus, ACC, left insula, left superior temporal gyrus, right anterior thalamic region and bilateral prefrontal cortex (PFC) (38–40). Nevertheless, CBMA is intrinsically limited by its focus on local spatial overlap. It treats each brain region as an independent unit, thereby overlooking the

functional embedding of these regions within large-scale brain networks (41). Consequently, the persistent heterogeneity in VBM literature may not reflect random noise, but rather structural alterations in distinct nodes that share a common dysfunctional circuit.

The network-based perspective reframes the disparate regional findings as interconnected nodes within a large-scale dysfunctional circuit (42–44). This perspective is particularly compelling for chronic smoking, as converging evidence from resting-state functional Magnetic Resonance Imaging (rs-fMRI) studies have found altered functional connectivity (FC) within networks such as the Default Mode Network (DMN), Salience Network (SN), and Executive Control Network (ECN) in chronic smokers (45–47). Crucially, many of the regions encompassed by these networks—such as the ACC, dorsolateral PFC, and insula—are also the same areas repeatedly identified in VBM analysis, providing a strong indication of a structure–function correspondence (22, 23, 28). Indeed, beyond smoking, the broader field of addiction science has increasingly coalesced around the view of addiction as a circuit-level disorder, with neuroimaging evidence implicating disruptions in the SN, ECN, and reward networks across various substance use and behavioral addictions (48, 49). To rigorously test whether the heterogeneous GM alterations in smokers conform to this circuit-level hypothesis, methodological advancements such as functional connectivity network mapping (FCNM) offer a unique analytical framework. FCNM allows for the precise mapping of focal structural coordinates onto distributed brain networks, which may guide targeted clinical interventions (e.g., neuro-modulation sites) (49–52). However, despite the strong theoretical rationale and the established utility of network mapping, a systematic FCNM-driven synthesis to reconcile the heterogeneous GM volume alterations reported in the chronic smoking literature has not yet been undertaken.

Therefore, to address the gap identified in the literature, the present study was designed with a threefold objective. First, we aimed to systematically characterize convergent regional GM alterations across prior whole-brain VBM studies of chronic smokers. Second, utilizing these localized peaks of structural alteration as seeds, we sought to identify the common functional brain networks associated with these changes. To achieve this, we employed a coordinate-based FCNM integrated with the large-scale Human Connectome Project (HCP) dataset. Third, to dissect the heterogeneity underlying these alterations, we performed subgroup analysis based on cumulative smoking exposure (pack-years) to elucidate potential dose-dependent trajectories of network dysregulation.

2 Materials and methods

2.1 Study search and selection

A comprehensive and systematic literature search was conducted across PubMed, Web of Science, and Embase to identify studies

examining brain GM differences between chronic smokers and non-smokers published prior to September 1, 2025. The following search terms were used: (“smoking” OR “smokers” OR “nicotine” OR “tobacco” OR “cigarette”) AND (“voxel” OR “VBM” OR “morphometry” OR “grey matter” OR “gray matter”). We also manually checked the reference lists of relevant reviews and meta-analysis to identify studies potentially missed by the database search.

The inclusion criteria were as follows: (1) original peer-reviewed articles published in English; (2) studies defining chronic smokers as individuals smoking at least five cigarettes daily; (3) studies employing VBM to compare GM differences between chronic smokers and non-smokers; (4) studies using significance thresholds corrected for multiple comparisons, or uncorrected thresholds with spatial extent correction; (5) studies reporting whole-brain VBM results as 3D coordinates (x , y , z) in Talairach or Montreal Neurological Institute (MNI) space.

The exclusion criteria were as follows: (1) pre-existing neuropsychiatric disorders (e.g., Parkinson’s disease, multiple sclerosis) or severe somatic disorders; (2) history of head injury with loss of consciousness, MRI contraindications, or a first-degree family history of psychiatric disorders. This study was conducted in accordance with the Preferred Reporting Items for Systematic Reviews and Meta-Analyses (PRISMA) 2020 guidelines, as illustrated in the selection flow diagram (Supplementary Figure S1) (53). Our analysis centered on the various comparisons within a single study, such as group comparisons between smokers and non-smokers in imaging patterns, rather than on the studies themselves.

Two independent reviewers extracted the peak coordinates (x , y , z) of significant gray matter volume differences between chronic smokers and non-smokers directly from the results tables or text of the included studies. We extracted all reported significant foci rather than selecting only the most significant one to maximize data coverage. To ensure spatial consistency across studies, coordinates originally reported in Talairach space were converted to MNI space using the Lancaster transform (icbm2tal) (54). This standardized set of MNI coordinates served as the input for the subsequent network mapping analysis.

2.2 Rs-fMRI dataset from HCP

This study utilized rs-fMRI data obtained from the HCP. The dataset included 1,093 healthy adults (594 females; mean age = 28.8, SD = 3.7 years), who were recruited at Washington University, primarily from families of twins and their non-twin siblings. To ensure data quality, participants with major radiological anomalies that could confound brain connectivity analysis were excluded. Participants with less severe focal abnormalities were not excluded but were documented with data flags on the HCP public wiki page (55). The age range for inclusion was limited to 22–35 years to enhance physiological and psychological stability in the sample, thus increasing the reliability and comparability of the results (55). Demographic information for the dataset is provided in Supplementary Table S1.

2.3 Rs-fMRI data acquisition and preprocessing

Rs-fMRI data from the HCP were collected on a 3 T Siemens Trio Scanner. The rs-fMRI acquisition parameters are detailed in Supplementary Table S2. Participants were excluded if their data

exhibited poor image quality (e.g., visible artifacts) or incomplete brain coverage.

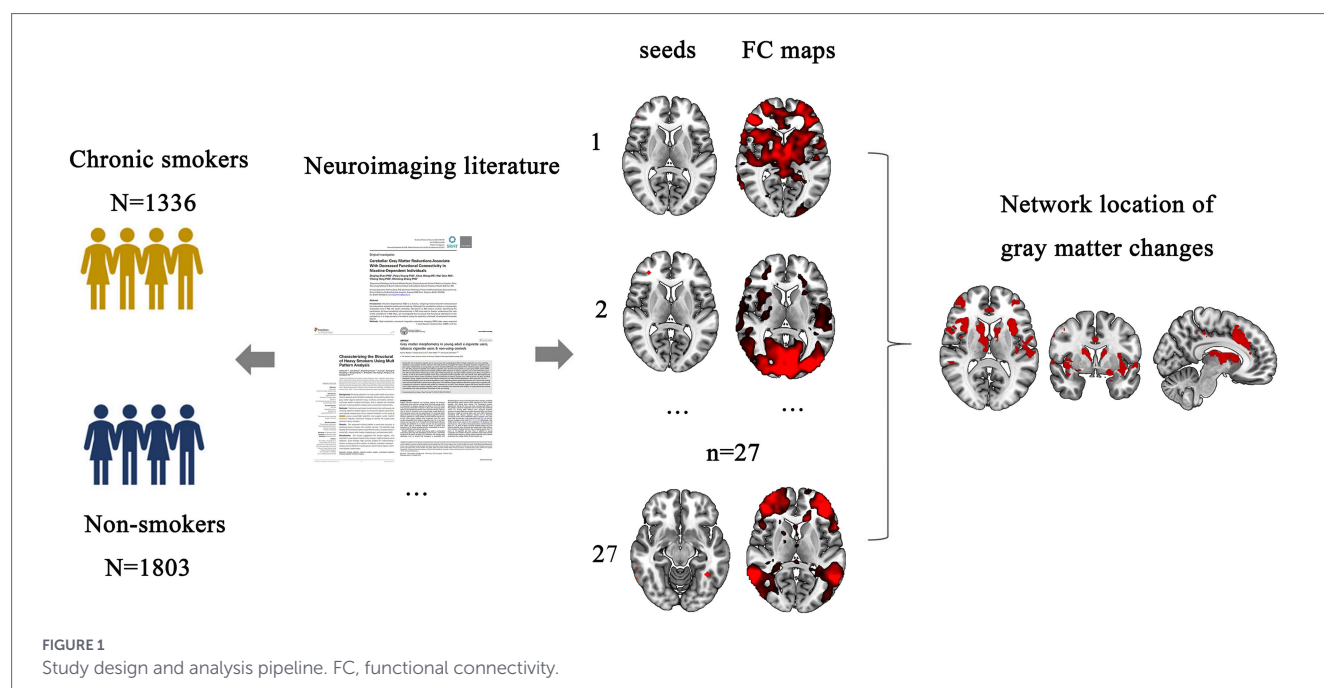
Rs-fMRI data preprocessing was performed utilizing Statistical Parametric Mapping 12 (SPM12; <https://www.fil.ion.ucl.ac.uk/spm/>) and the Data Processing & Analysis for Brain Imaging (DPABI; <https://rfmri.org/DPABI>) toolbox (56). The initial 10 volumes were excluded for each participant to achieve signal stability and participant acclimatization. The remaining volumes underwent slice-time correction and were then realigned to address head motion. The realignment process produced six motion parameters, comprising three translations and three rotations, for each volume. All participants’ data met the predetermined quality control standards for head motion, with maximal translation and rotation both below 2 mm and 2°, respectively. In order to enhance head motion control, framewise displacement (FD) was initially computed for each participant. A comprehensive nuisance regression was conducted subsequently to eliminate various confounding variables, including the linear trend, the 24 Friston motion parameters, signals from white matter and cerebrospinal fluid, and individual volumes flagged as motion outliers (FD > 0.5 mm). Global signal regression was incorporated in this step to enhance the detection of large-scale network correlations and to improve correspondence with structural connectivity (57). The datasets were subjected to bandpass filtering, preserving frequencies ranging from 0.01 to 0.1 Hz. The first stage of spatial normalization entailed co-registering the T1-weighted structural image of each participant with their average functional image. The structural images were transformed, segmented, and normalized to MNI space. Each filtered functional volume was then spatially normalized to MNI space. Finally, all functional data underwent spatial smoothing with a Gaussian kernel of $6 \times 6 \times 6$ mm³ full-width at half maximum.

2.4 FCNM analysis

To investigate brain networks linked to smoking-related structural GM volume alterations, we employed the FCNM approach. This method used coordinates of GM differences between chronic smokers and non-smokers as seeds. We delineated the functional network linked to smoking-induced GM changes using a five-step seed-based connectivity analysis implemented in MATLAB version 9.5 (R2018b). A schematic overview of the study design and analysis pipeline is provided in Figure 1. First, we formed a seed by creating 4-mm radius spheres centered on the peak coordinates identified in a previous structural analysis and consolidating them into a unified composite mask. Second, using rs-fMRI data from 1,093 HCP participants, individual seed-to-whole-brain FC maps were computed by calculating Pearson’s correlations between mean time course of the seed and every other brain voxel, followed by a Fisher’s z -transformation. Third, a group-level, one-sample t -test was conducted on the individual FC maps. This analysis focused solely on positive correlations due to the uncertain neurophysiological implications associated with negative FC (57, 58). Fourth, group t -maps were binarized at $p < 0.05$, following thresholding and correction for multiple comparisons using voxel-level false discovery rate. Finally, binarized FC maps were overlaid, and then thresholded at a 50% probability to create the ultimate smoking-related GM alteration network.

2.5 Association with canonical brain networks

To ascertain its functional significance, we mapped the smoking-related alteration network onto a canonical functional atlas



comprising 14 established resting-state networks (59), thereby quantifying its spatial distribution across these systems. These canonical networks encompassed: anterior SN, left ECN (LECN), right ECN (RECN), basal ganglia network, ventral DMN (vDMN), language network, sensorimotor network, auditory network, posterior SN, visuospatial network, dorsal DMN (dDMN), precuneus network, high visual network, and primary visual network (59). The spatial association degree was determined by quantifying the percentage of voxels within each canonical network that showed spatial overlap with the smoking-related brain alteration network.

2.6 Subgroup analysis

To explore the potential heterogeneity of smoking-related network alterations and verify the robustness of our findings, we conducted subgroup analysis based on cumulative tobacco exposure. Studies were stratified into higher-exposure ($n = 8$) and lower-exposure ($n = 8$) smoking groups using the median pack-years as the cutoff value. Separate FCNM analysis were performed for each subgroup using the standard 4-mm radius. Within each subgroup, binarized FC maps were overlaid and applied a 60% threshold to define the consensus smoking-related GM alteration network. To further confirm the stability of these subgroup-specific findings, we also repeated the FCNM procedure using 1-mm and 7-mm radius spheres as sensitivity analysis.

3 Results

3.1 Included studies

Following a systematic literature search and selection process, our analysis incorporated 27 studies and 36 contrasts, representing data from 1,336 chronic smokers and 1803 non-smokers. There were no

statistically significant differences between chronic smokers and non-smokers in average sample size ($p = 0.22$) or gender distribution (relative risk = 0.94, 95% CI = 0.87 to 1.02, $z = -1.53$, $p = 0.127$). Participants smoked an average of 17.32 ± 10.00 cigarettes per day, with a mean smoking history of 14.69 ± 11.99 pack-years. The average Fagerström Test for Nicotine Dependence (FTND) score was 4.96 ± 2.38 , indicating moderate nicotine dependence. Other imaging characteristics of the included studies are summarized in Table 1.

3.2 Chronic smoking-related GM volume networks

The FCNM method revealed that the smoking-related GM alteration networks encompassed a distributed set of brain regions, prominently including the supramarginal gyrus (SMG), insula, ACC, caudate nucleus, putamen, and superior temporal gyrus (STG) (Figure 2). Spatial overlap analysis with canonical networks indicated that the chronic smoking-related network primarily involved the posterior SN (51.59%), anterior SN (32.15%), basal ganglia network (31.52%), and auditory network (24.19%) (Figure 3). Lower percentages of overlap were observed for other networks, including the LECN (1.85%), RECN (0%), vDMN (0%), language network (3.18%), sensorimotor network (6.98%), visuospatial network (0.21%), dDMN (0.37%), precuneus network (0.06%), high visual network (0%), and primary visual network (4.06%) (Figure 3). To confirm the robustness of these findings, we conducted sensitivity analysis by repeating the FCNM procedure with different seed radii. The brain alteration networks generated using 1-mm (Supplementary Figure S2) and 7-mm (Supplementary Figure S3) radius spheres were spatially highly similar to the network identified in the primary 4-mm analysis. Furthermore, a quantitative overlap analysis was performed for each sensitivity network. The analysis for the 1-mm radius network (Supplementary Figure S4) demonstrated that the posterior Salience, anterior Salience, basal ganglia, and auditory networks were the most predominantly involved systems. A highly consistent pattern was

TABLE 1 Demographic and clinical characteristics, and technical information of VBM studies included in the study.

Study	Sample (female)	Age (SD)	Smoking History (SD)	Cigarette/ day (SD)	Pack-years	FTND	Threshold	Software
Almeida et al. (2011) (164)	CS39 (25) NS39 (Na)	75.0 (3.4) 75.7 (3.2)	59 (Na)	25(Na)	Na	4 (Na)	$p < 0.005$ uncorrected	SPM2
Boparai et al. (2025) (165)	CS26 (9) NS25 (10)	22.15 (1.95) 22.36 (2.02)	5.23 (2.64)	8.24 (5.47)	Na	2.58 (2.18)	$p < 0.05$ corrected	SPM12
Brody et al. (2004) (111)	CS19 (11) NS17 (10)	39.5 (10.3) 37.9 (12.9)	31.0 (17.9)	26.2 (7.4)	Na	5.1 (1.9)	$p < 0.001$ uncorrected	SPM99
Bu et al. (2016) (22)	CS26 (0) NS26 (0)	21.42 (1.73) 20.58 (1.47)	4.27 (2.44)	15.04 (4.82)	3.55 (2.97)	4.42 (2.20)	$p < 0.05$ corrected	SPM8
Cai et al. (2022) (21)	CS23 (6) NS23 (6)	45.7 (6.8) 43.8 (9.4)	23.8 (7.9)	Na (Na)	Na	8.89 (0.71)	$p < 0.05$ corrected	SPM8
Chen et al. (2022) (166)	CS70 (29) NS209 (80)	29.79 (3.05) 29.54 (3.41)	15.14 (3.34)	Na	Na	4.83 (0.88)	$p < 0.001$ uncorrected	SPM
Conti et al. (2021) (20)	CS28 (10) NS24 (11)	28.1 (8.3) 28.5 (9.5)	Na	15.0 (4.5)	10.4 (8.1)	5.0 (1.5)	$p < 0.05$ corrected	SPM12
Daniju et al. (2022) (167)	CS19 (14) NS35 (20)	22.8 (3.6) 22.8 (4.9)	6.2 (4.2)	6.6 (5.3)	2.7 (3.65)	Na	$p < 0.05$ corrected	SPM12
Faulkner et al. (2021) (168)	CS12 (8) NS26 (15)	25.40 (4.58) 22.87 (4.60)	Na	11.45 (4.73)	6.21 (5.37)	Na	$p < 0.001$ corrected	SPM12
Franklin et al. (2014) (24)	CS80 (39) NS80 (39)	33.8 (Na) 22.1 (Na)	14.1 (Na)	14.7 (Na)	10.5 (Na)	4.45 (Na)	$p < 0.025$ corrected	SPM8
Fritz et al. (2014) (28)	CS315 (167) NS659 (416)	44.10 (11.84) 51.49 (14.45)	26.8 (Na)	13.17 (6.99)	17.81 (12.25)	Na	$p < 0.05$ corrected	SPM8
Gallinat et al. (2006) (26)	CS22 (12) NS23 (12)	30.8 (7.5) 30.3 (7.9)	13.9 (7.3)	14.5 (9.2)	13.5 (13.0)	2.9 (1.7)	$p < 0.05$ corrected	SPM2
Hanlon et al. (2016) (23)	CS58 (25) NS60 (27)	31.7 (Na) 29.7 (Na)	15.5 (Na)	16.2 (Na)	12.2 (Na)	4.6 (Na)	$p < 0.01$ corrected	SPM8
Kunas et al. (2020) (169)	CS62 (34) NS116 (67)	31.23 (9.5) 31.85 (10.8)	Na	Na	Na	Na	$p < 0.001$ uncorrected	SPM12
Liao et al. (2010) (170)	CS44 (36) NS44 (34)	28.1 (5.5) 26.3 (5.8)	10.4 (5.7)	20.3 (7.7)	Na	Na	$p < 0.05$ corrected	SPM5
Morales et al. (2012) (171)	CS25 (13) NS18 (8)	35.4 (1.8) 30.1 (2.2)	19 (Na)	14.1 (1.2)	11.5 (1.9)	3.8 (0.4)	$p < 0.05$ corrected	SPM8

(Continued)

TABLE 1 (Continued)

Study	Sample (female)	Age (SD)	Smoking History (SD)	Cigarette/ day (SD)	Pack-years	FTND	Threshold	Software
Peng et al. (2015) (19)	CS26 (0) NS53 (0)	29.42 (4.43) 30.83 (5.18)	Na	16.15 (5.16)	8.77 (3.57)	Na	$p < 0.05$ corrected	SPM8
Peng et al. (2015) (19)	CS27 (0) NS53 (0)	32.26 (3.73) 30.83 (5.18)	Na	38.70 (8.36)	31.06 (7.40)	Na	$p < 0.05$ corrected	SPM8
Qian et al. (2019) (172)	CS44 (Na) NS41 (Na)	39 (6.5) 38.5 (7.4)	18.9 (6.4)	23.6 (10.4)	Na	5.4 (2.4)	$p < 0.01$ corrected	SPM8
Shen et al. (2018) (32)	CS85 (0) NS41 (0)	38.24 (6.81) 38.46 (8.60)	17.36 (6.58)	23.46 (9.53)	20.63 (12.28)	5.18 (2.18)	$p < 0.05$ corrected	SPM8
Stoeckel et al. (2016) (78)	CS16 (4) NS16 (5)	37.94 (11.61) 34.19 (7.20)	17.63 (10.49)	16.00 (4.84)	16.09 (12.17)	4.44 (2.16)	$p < 0.05$ corrected	SPM8
Wang et al. (2014) (25)	CS22 (0) NS20 (0)	22.48 (2.48) 21.80 (1.32)	4.95 (2.27)	11.90 (6.13)	3.10 (2.63)	Na	$p < 0.05$ corrected	SPM8
Weidler et al. (2024) (173)	CS52 (Na) NS45 (Na)	26.08 (6.91) 27.16 (6.15)	8.93 (7.89)	12.32 (4.48)	Na	3.72 (2.18)	$p < 0.05$ corrected	SPM
Weng et al. (2022) (174)	CS67 (Na) NS43 (Na)	29.22 (6.36) 29.51 (5.85)	Na	Na	Na	4.65 (1.76)	$p < 0.05$ corrected	SPM8
Ye et al. (2021) (175)	CS37 (8) NS28 (8)	47.18 (7.22) 43 (9.62)	25.34 (9.23)	35.13 (10.70)	Na	8.89 (0.68)	$p < 0.05$ corrected	SPM8
Yu et al. (2011) (29)	CS16 (Na) NS16 (Na)	41.6 (5.5) 39.2 (4.5)	21.1 (3.9)	20.6 (7.4)	Na	7.19 (1.42)	$p < 0.05$ corrected	SPM5
Zhang et al. (2022) (30)	CS28 (Na) NS28 (Na)	31.29 (5.56) 31.68 (6.57)	11.82 (5.77)	16.11 (8.35)	10.08 (7.95)	3.54 (2.03)	$p < 0.001$ corrected	SPM12
Zhang et al. (2011) (27)	CS48 (24) NS48 (24)	31.4 (8.1) 31.1 (8.8)	12.8 (7.4)	20.19 (6.6)	12.9 (7.9)	5.4 (1.9)	$p < 0.05$ corrected	FSL

VBM, voxel-based morphometry; Na, not available; FTND, Fagerstrom test of nicotine dependence; CS, chronic smokers; NS: non-smokers; SPM, statistical parametric mapping; FSL, functional magnetic resonance imaging of the brain software library.

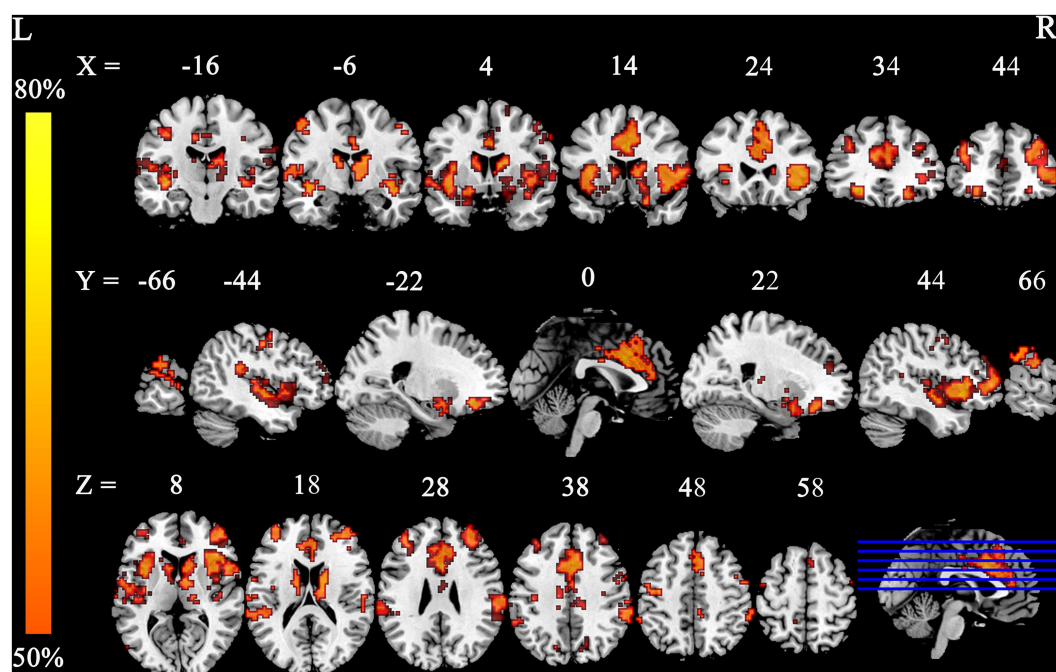


FIGURE 2

Smoking-related GM alteration networks based on 4 mm radius sphere. Smoking-related GM alteration networks are shown as network probability maps thresholded at 50%, showing brain regions functionally connected to more than 50% of the contrast seeds.

observed in the analysis for the 7-mm radius network (Supplementary Figure S5), which also identified these same networks as having the highest overlap. These results confirm the stability of our primary findings across different analytical parameters.

3.3 Subgroup analysis

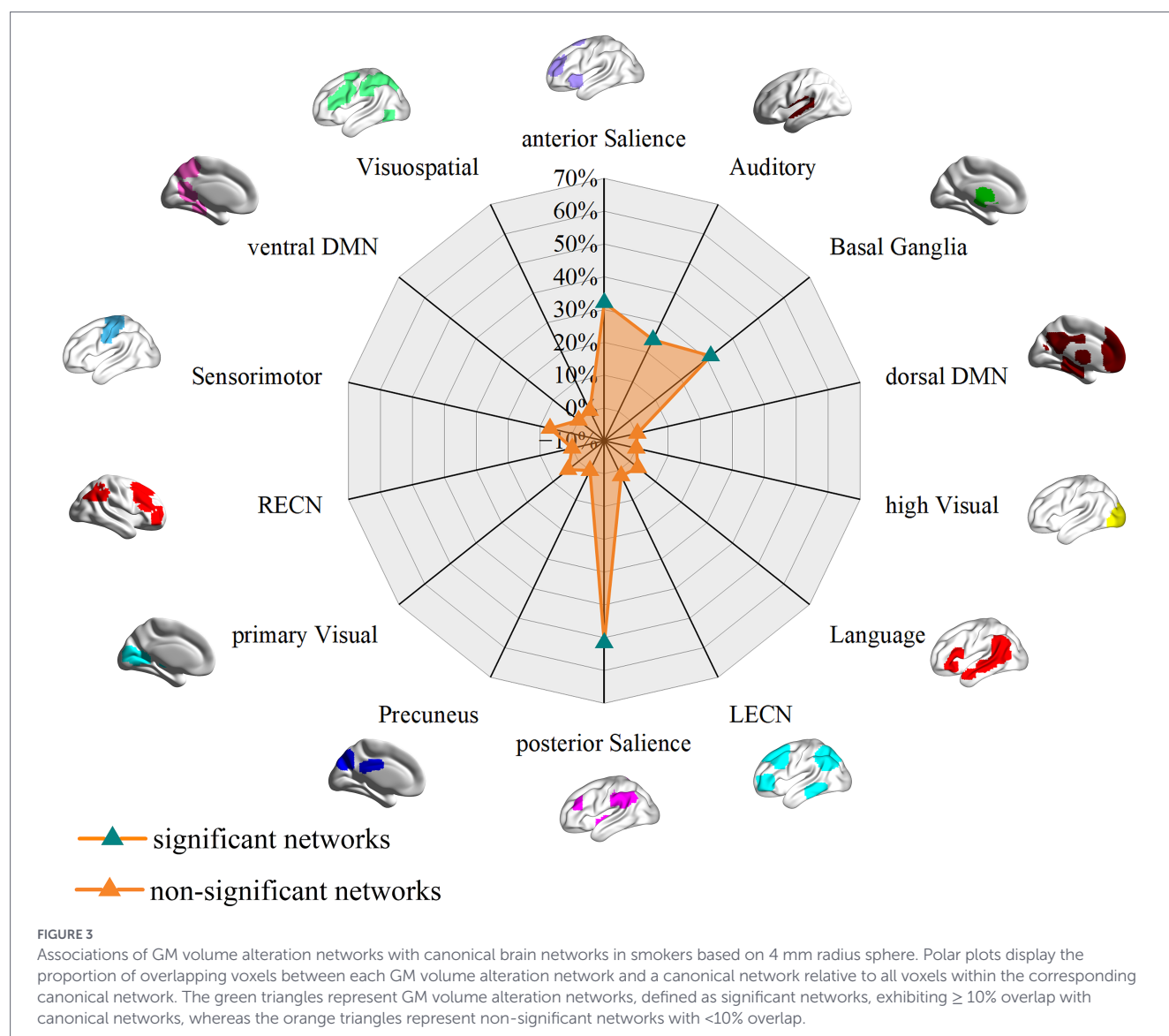
To investigate the impact of cumulative tobacco exposure on network alterations, we stratified the included studies reporting pack-year information into higher-exposure ($n = 8$) and lower-exposure ($n = 8$) subgroups using the median value as the cutoff. Detailed characteristics of the included studies for each subgroup are provided in Supplementary Tables S3, S4. FCNM analysis revealed that both subgroups exhibited alteration patterns largely overlapping with the main findings, particularly involving the posterior and anterior SN and the basal ganglia network (Figures 4, 5). However, notable differences were observed the higher-exposure subgroup demonstrated more extensive involvement of the vDMN (Figure 4), whereas the auditory network showed negligible alterations in the lower-exposure subgroup (Figure 5). The specific anatomical regions corresponding to these distinct network patterns are detailed in Figures 6, 7. To verify the robustness of these subgroup-specific findings, we conducted sensitivity analysis by repeating the FCNM procedure using 1-mm (Supplementary Figures S6–S9) and 7-mm (Supplementary Figures S10–S13) radius spheres. The resulting network patterns were highly consistent with those identified using the primary 4-mm radius, confirming the stability of our subgroup results across different analytical parameters. These results suggest a potential dose-dependent effect of smoking on brain network integrity.

4 Discussion

This study utilized the FCNM approach and a large-scale human connectome dataset to elucidate smoking-related GM alterations at the network level. The identified smoking-associated GM alteration networks encompassed spatially distributed brain regions, predominantly involving the posterior SN (pSN), anterior SN (aSN), basal ganglia network, and auditory network. The robustness of the FCNM was demonstrated by reproducing it with varying radii (1-mm and 7-mm). These findings provide empirical evidence for network-level GM alterations in chronic smokers, enhancing our understanding of the neuropathophysiological mechanisms of smoking addiction from a network perspective and potentially guiding the development of targeted interventions for it.

4.1 Abnormal pSN and aSN in smokers

The SN, particularly its posterior component, exhibited significant disruption in the smokers identified in our study. The pSN, including the SMG identified as an important node in our study, plays a crucial role in task switching, attention distribution, and the coordination of behavioral control (60–62). Consistent with the disruption, rs-fMRI analysis has shown a trend of decreased FC in the pSN of chronic smokers compared to non-smokers, a deficit often associated with cognitive impairment (63, 64). The aSN was also found to be involved in the network of GM alterations associated with smoking. This network, centered on the anterior insula and dorsal ACC, is vital for salience detection, executive functions, and emotional regulation (65–68). Our findings align with rs-fMRI studies that have reported reduced FC within the aSN in smokers, a finding that has also been linked to severity of nicotine addiction (69–72).



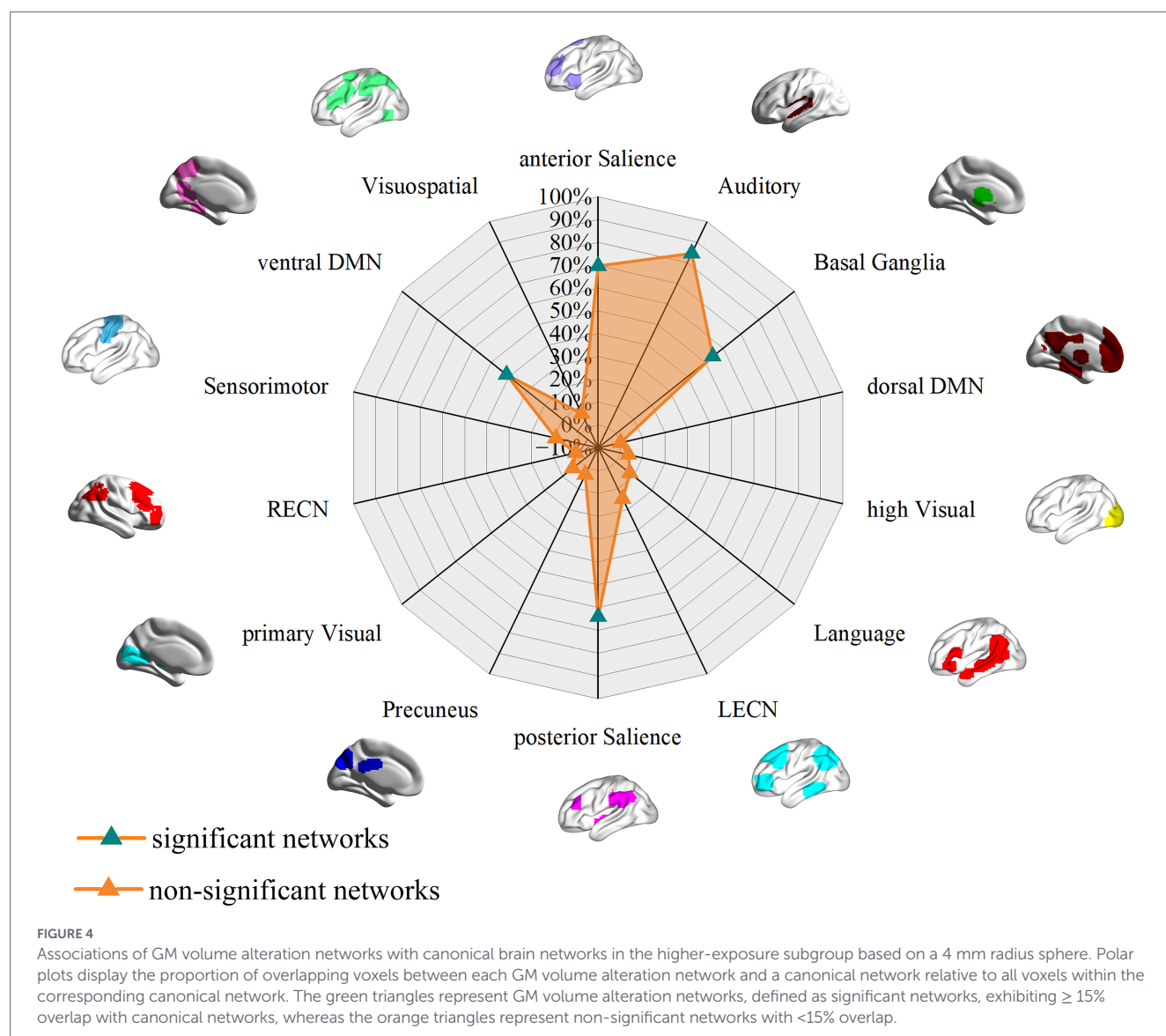
The SMG, identified as a critical node of pSN, displayed noteworthy structural and functional changes of chronic smokers in recent studies (29, 73–75). Reduced FC was noted between the SMG and prefrontal regions (76), alongside sex-specific connectivity patterns associated with the basal nucleus of Meynert (74). Moreover, smokers exhibited notably reduced regional cortical perfusion in the right SMG compared to non-smokers (77).

Within the aSN, converging evidence from VBM studies consistently indicates altered GM volume and density in the anterior insula of smokers (19, 25–27), which is negatively correlated with daily cigarette consumption (78). Crucially, damage to the anterior insula diminishes cravings, providing compelling evidence for its causal role in addiction (79). In line with this structural and causal evidence, rs-fMRI unequivocally demonstrates altered anterior insula function, manifesting as heightened reactivity to negative stimuli, particularly in heavier smokers, and weakened anterior insula-ACC connectivity associated with dependence (80–84). The anterior insula, being a central hub in the triple network (SN-central executive network-DMN) and exerting significant influence over impulse control and craving, emerges as a key candidate for therapeutic interventions (85–90). Similarly, the dorsal ACC, a key partner of the anterior insula within

the aSN (65), also displays marked abnormalities in chronic smokers. Event-related potential and VBM studies converge to reveal inhibitory control deficits and reduced GM volume in the dorsal ACC (21, 22, 28, 91). Moreover, fMRI-based neurofeedback and abstinence studies have demonstrated significant disruptions in ACC activity and connectivity patterns in chronic smokers, which are associated with craving, cognitive impairments, and heightened risk of relapse (92–95). Notably, interventions such as integrative body–mind training and mindfulness-based therapies have the potential to regulate dorsal ACC activity, thereby enhancing smoking cessation results (96, 97), thus solidifying the position of dorsal ACC as a crucial therapeutic target within the SN (98).

4.2 Abnormal basal ganglia network in smokers

The basal ganglia network is acknowledged for its essential involvement in various functions, encompassing motor learning, executive functions, behavioral regulation, and emotional processing (99). Crucially, it is central to reward processing and plays a significant role in smoking addiction (100–102). Converging evidence from



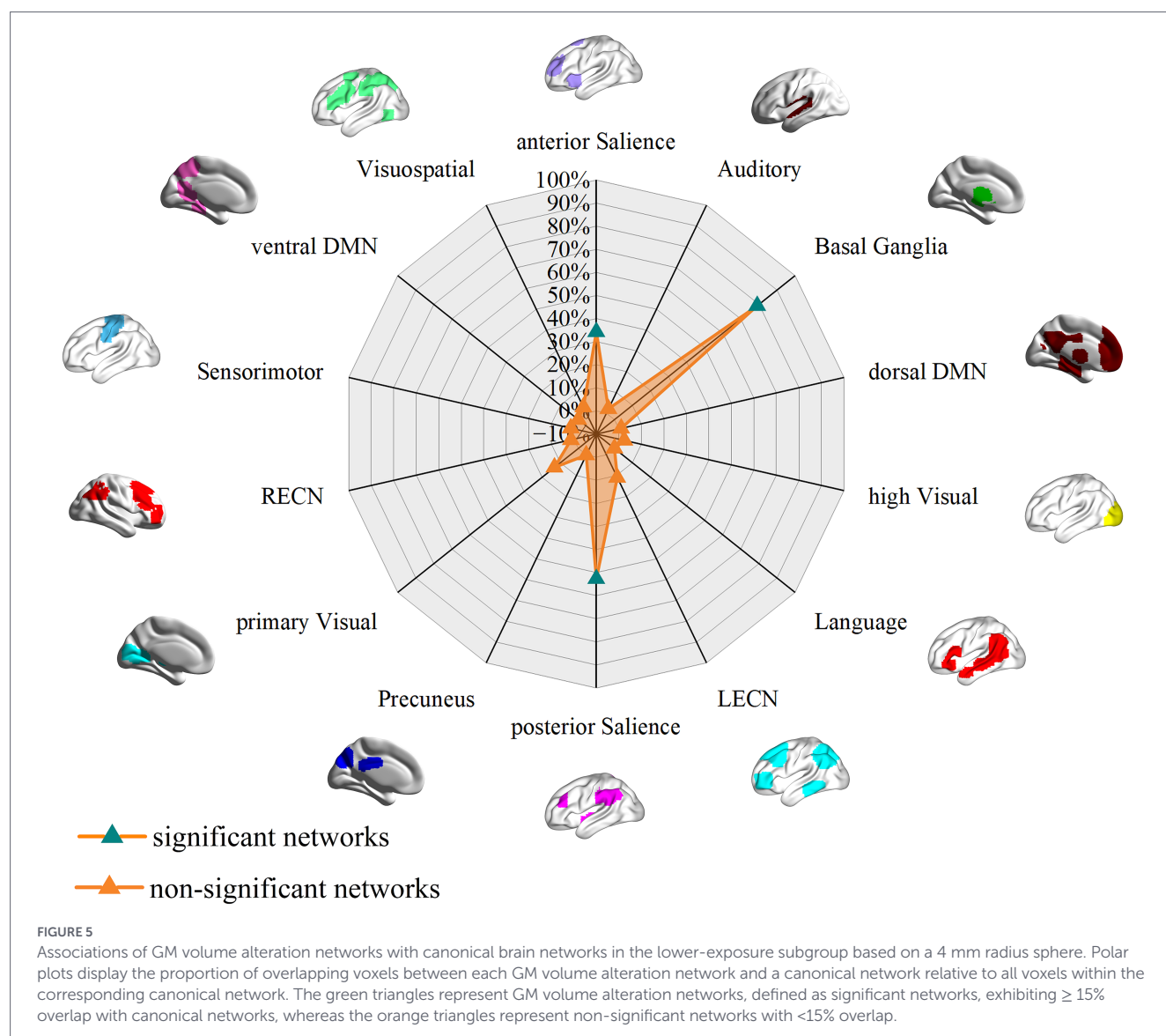
multiple neuroimaging modalities reveals the underlying mechanisms at different levels (80, 103–105). First, at the neurochemical level, positron emission tomography (PET) studies have demonstrated that smoking disrupts dopamine activity within the basal ganglia network, leading to a cascade of neural adaptations that encompass altered reward responses, activation of stress-related systems, and impaired cognitive control, all of which contribute to the maintenance and intensification of nicotine addiction (103). Second, rs-fMRI studies consistently show reduced FC between basal ganglia regions (such as the caudate and putamen) and other brain areas (80). Furthermore, dynamic FC analysis reveal that this network dysfunction is not static; instead, it involves dynamic changes that heighten the sensitivity of the reward system, thereby promoting the maintenance of smoking behavior (104, 105). Together, these findings firmly establish the basal ganglia network as a critical hub in addictive smoking behaviors.

As core components of the basal ganglia network, the striatum (primarily the caudate nucleus and putamen) plays a pivotal role in cognition, learning, and motivation, and its dysfunction has been consistently implicated in smoking addiction (76, 106, 107). Converging neuroimaging evidence reveals widespread functional abnormalities within the striatum of smokers. For instance, functional Magnetic

Resonance Imaging (fMRI) and PET studies have identified reduced FC and diminished cerebral blood flow in the caudate nucleus (76, 108, 109). Similarly, the putamen exhibits altered FC with regions like the insula, alongside dopamine-related abnormalities (110, 111). Underlying these functional alterations is a profound neurochemical imbalance. Research shows that dopamine dysregulation in the striatum reinforces nicotine addiction (80, 111, 112), whereas modulating striatal dopamine and FC of striatum may facilitate nicotine withdrawal. This not only highlights the importance of striatum in the addiction mechanism but also underscores its potential as a therapeutic target. Therefore, targeting the striatum and the broader basal ganglia network with interventions such as deep brain stimulation or repetitive transcranial magnetic stimulation shows significant promise, offering a key direction for the development of effective smoking cessation therapies (100, 104, 113–115).

4.3 Abnormal auditory network in smokers

While the roles of the pSN, aSN, and basal ganglia network in smoking-related neurobiological changes are well-documented, research on the auditory network remains limited. The lack of research



on this topic raises important questions about its potential role in the neurobiology of smoking behavior, possibly influencing cue-induced reactivity or sensory integration within the auditory network (116, 117).

The auditory network is mainly tasked with processing auditory information and associated cognitive functions, thereby playing a crucial role in environmental interactions (118, 119). Despite its lesser established role in core addiction processes like reward when compared to the basal ganglia network, the auditory system may potentially influence smoking behavior through pathways related to cue reactivity or altered sensory processing, in conjunction with recognized clinical connections between smoking and hearing impairment (116, 117, 120–122). Neuroimaging evidence increasingly suggests structural and functional alterations in the auditory network, particularly within the STG, among chronic smokers (19, 26, 123, 124).

The STG is primarily associated with auditory processing and cross-modal integration (125–127). Structural investigations in smokers consistently reveal abnormalities in this region, characterized by altered GM volume/density and cortical thinning in the STG (19, 26, 128–130). Altered intrinsic activity in the STG and decreased FC have been observed in complementary rs-fMRI studies, which are

associated with nicotine intake, severity of dependence, relapse, impulsivity, and impaired control (123, 124). Task-fMRI showed heightened STG reactivity to smoking cues (131–133), and arterial spin labeling MRI demonstrated reduced STG perfusion in smokers (77). Taken together, these findings highlight the auditory network, particularly the STG, as being affected by chronic smoking. The auditory network alteration may serve as a neural marker and potential predictor of cessation outcomes (123). Despite historical under-emphasis, considering the auditory network is crucial for future smoking research and intervention development.

4.4 Subgroup analysis

Our subgroup analysis stratified by pack-years provided critical insights into the potential dose-dependent nature of smoking-related network alterations. First, the SN and basal ganglia network were consistently identified in both higher- and lower-exposure subgroups. This suggests that structural vulnerabilities in these systems—which are important for attention distribution, emotional processing and reward processing—represent the core neuropathology of nicotine addiction (60–62, 99–102). These alterations likely emerge relatively

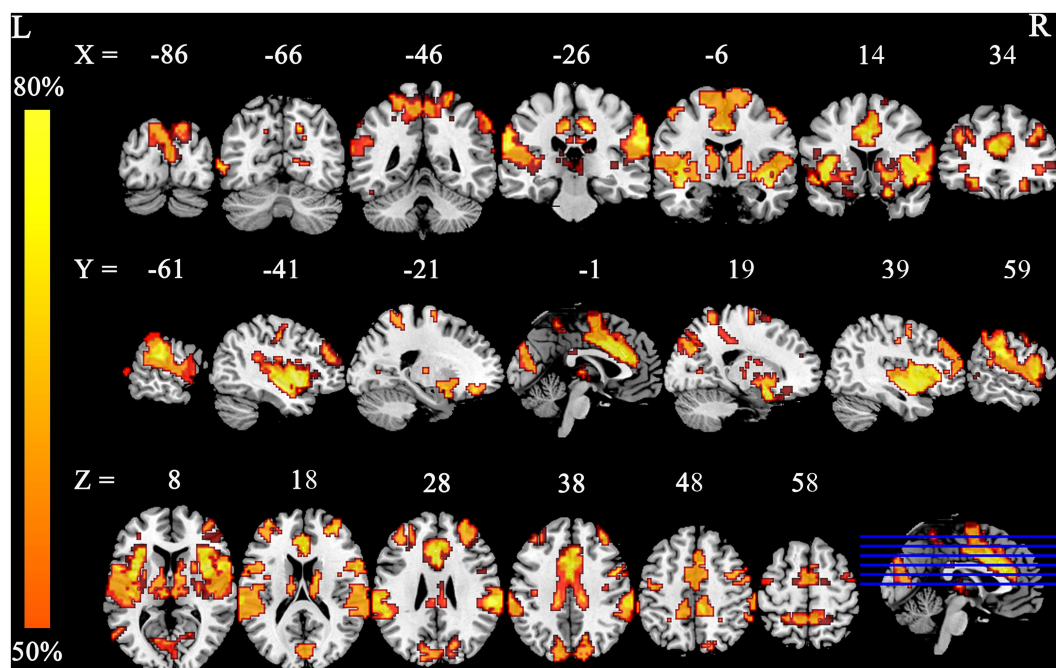


FIGURE 6

Smoking-related GM alteration networks in the higher-exposure subgroup based on a 4 mm radius sphere. Smoking-related GM alteration networks are shown as network probability maps thresholded at 60%, showing brain regions functionally connected to more than 60% of the contrast seeds.

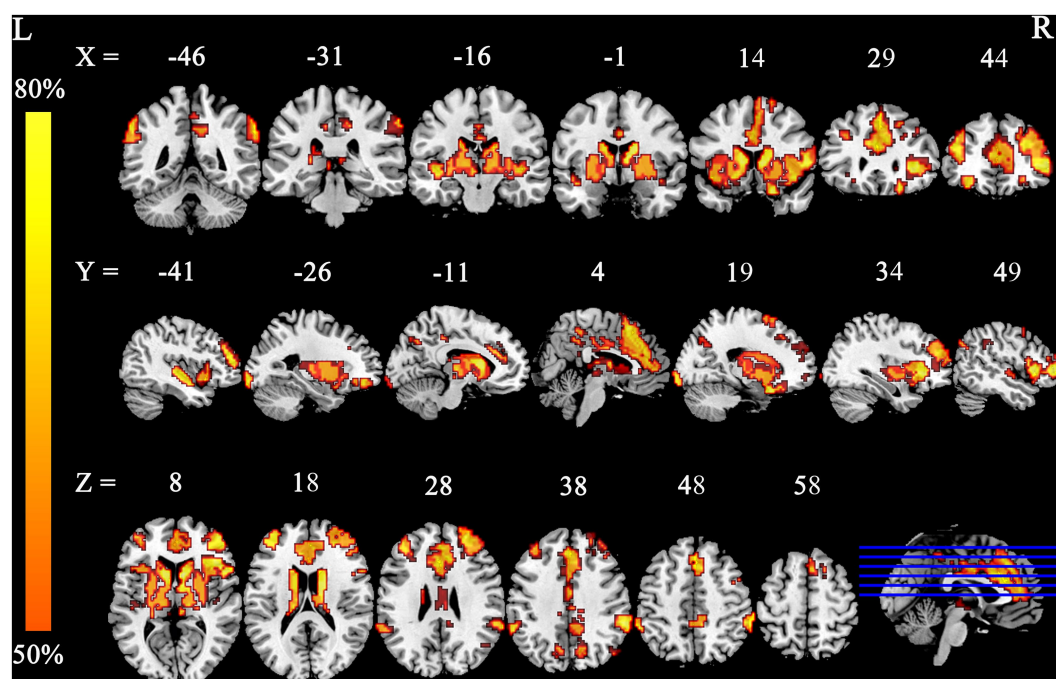


FIGURE 7

Smoking-related GM alteration networks in the lower-exposure subgroup based on a 4 mm radius sphere. Smoking-related GM alteration networks are shown as network probability maps thresholded at 60%, showing brain regions functionally connected to more than 60% of the contrast seeds.

early in the addiction trajectory and persist throughout the course of the disorder. Second, a notable divergence was observed in the vDMN, characterized by extensive involvement specifically within the higher-exposure group. While the DMN is primarily implicated in self-referential processing and episodic memory (134), recent literature indicates that greater nicotine dosage and duration drive significant

functional and structural alterations within this network, including altered regional homogeneity and efficiency (75, 130, 135–137). Crucially, within this dysregulated vDMN, the Inferior Parietal Lobule (IPL) may serve as a pivotal hub particularly vulnerable to these exposure-related alterations. As a heteromodal association hub integrating sensory inputs with internal memory representations (138, 139), the

IPL in smokers shows exposure-related cortical thinning and heterogeneous functional-dynamic alterations with the insula (137, 140–142). Collectively, these findings suggest a hemispheric lateralization of control failure: reduced dynamic flexibility in right frontoparietal regions creates a neural shortcut where smoking cues bypass executive oversight, directly activating automated approach tendencies (61, 142, 143). This transition from goal-directed to habitual control is evidenced by reduced effective connectivity from parietal nodes to the medial PFC, functionally disconnecting executive oversight and allowing drug cues to bypass conscious deliberation (135, 144–146). This mechanism may help explain why higher pack-years are associated with greater behavioral automaticity in smoking: we hypothesize that the IPL serves as a sensitized gateway that preferentially processes nicotine-associated stimuli. Furthermore, Hyper-synchrony of the posterior DMN and impaired switching to the executive control network likely underlie attentional bias and cognitive inflexibility in chronic smokers (147, 148). Consequently, therapeutic interventions such as repetitive transcranial magnetic stimulation and mindfulness-based neurofeedback should specifically targeting DMN nodes including the IPL to downregulate DMN hyperconnectivity of chronic smokers and restore the balance between internal rumination and external attention (145, 149–151). Third, the auditory network showed negligible structural alterations in the lower-exposure group, despite being prominent in the main analysis and higher-exposure group. This implies that structural deficits in primary sensory processing regions might be a cumulative, late-stage consequence of chronic neurotoxicity or vascular damage associated with long-term smoking, rather than a predisposing factor for addiction (130). Finally, the high spatial consistency of these subgroup-specific patterns across different seed radii (1-mm, 4-mm, and 7-mm) reinforces the robustness of these findings, suggesting that the observed exposure-dependent distinctions reflect genuine biological heterogeneity rather than methodological artifacts.

4.5 Limitations and future perspectives

This study has several limitations that should be considered when interpreting the findings. First, the analysis depends on coordinate-based data extracted from published studies, which provides a summary statistic (peak location) and inherently loses spatial information compared to analysis using full statistical maps or individual participant data (50, 152–154). This coordinate-based approach is correlational and thus cannot establish causality between the identified network and smoking-related GM alterations (43). Future work integrating causal data, such as lesion network mapping studies relevant to addiction (49), could strengthen the interpretation. Second, considerable heterogeneity is observed among the included studies in terms of sample characteristics (e.g., smoking duration, severity, and demographics), imaging acquisition parameters, preprocessing pipelines, and statistical approaches (24, 155). Although FCNM aims to identify convergence amidst variability, the noise and biases introduced by this heterogeneity can obscure the discovery of a common network (50, 152). Furthermore, our FCNM analysis did not weight studies by sample size or effect size, as there is currently no universally accepted method for incorporating these criteria. Third, we utilized a normative connectome derived from healthy adults (HCP dataset) to map the networks associated with smoking-related GM alterations. This approach aligns with standard network mapping practices, where

evidence indicates that sample selection has minimal impact on network localization (43, 50, 153, 156–159). However, this method may introduce bias or reduce precision due to age or ethnic differences between the populations. Although a smoking-specific connectome might yield slight variations, research suggests such differences are negligible (49). Fourth, the study's retrospective design necessitates prospective validation of the identified smoking-related network in independent cohorts of smokers and non-smokers. Additionally, our exclusion of individuals who had quit smoking constrained our ability to assess the reversibility of the identified network alterations following cessation. Fifth, methodological choices, such as the radius of the coordinate spheres (although sensitivity analysis demonstrated robustness) and the probability threshold (set at 50%) used to define the final network, are important parameters that can influence the results (50, 160). The exploration of alternative parameters for additional insights was not within the scope of this initial network localization. Sixth, we identified a network linked to GM alterations in smokers; however, we did not conduct formal specificity testing to compare this network with those derived from coordinates associated with other conditions, such as other substance use disorders, aging, or other psychiatric conditions, as performed in certain network mapping studies (152, 160). Such comparisons would enhance assertions regarding the distinctiveness of the identified network in relation to smoking. Seventh, the subgroup analysis regarding smoking severity were constrained by the limited availability of detailed pack-year data in the included studies. Although we successfully stratified a subset of studies to explore dose-dependent effects, this classification relied on the reported mean pack-years for each study cohort. Consequently, this aggregate measure masks intra-sample heterogeneity, as individual participants within the same study likely exhibited wide variations in exposure levels above or below the mean. Furthermore, the reduced sample size in each subgroup ($n = 8$) may limit statistical power compared to the main analysis. Additionally, the potential collinearity between age and cumulative smoking exposure (pack-years) poses a challenge in fully disentangling their independent contributions to network alterations (161). Future studies utilizing individual-level data with large samples and prospective longitudinal designs are needed to precisely dissociate the effects of aging from chronic nicotine toxicity (162, 163). Finally, our findings should be viewed within the context of the persistent challenges affecting reproducibility in neuroimaging, including small sample sizes, clinical heterogeneity, experimental variability, and analytical flexibility (24, 34, 37). Continued efforts towards standardization, larger sample sizes, and transparent reporting are crucial for advancing the field.

5 Conclusion

In conclusion, this study adeptly applied the FCNM method, utilizing human connectome data, to synthesize the findings from previous VBM studies of chronic smokers that reported heterogeneous neuroanatomical changes. We identified consistent brain networks associated with smoking-related GM alterations, primarily encompassing regions within the pSN/aSN, basal ganglia network, and auditory network. Crucially, our subgroup analysis revealed an exposure-dependent expansion of neuropathology:

while core control systems (Salience and basal ganglia networks) are consistently affected, structural deficits progressively recruit the auditory network and vDMN in individuals with higher cumulative smoking exposure. These findings provide robust, network-level evidence for the structural impact of chronic smoking on the brain. By demonstrating that seemingly disparate regional findings converge onto specific functional networks, this work helps reconcile inconsistencies in the prior literature and significantly extends our understanding of the neuropathology of smoking from a systems perspective. The identification of these smoking-related networks provides valuable insights that could inform the development of more targeted and effective smoking cessation programs and prevention strategies.

Data availability statement

The original contributions presented in the study are included in the article/[Supplementary material](#), further inquiries can be directed to the corresponding authors.

Ethics statement

The studies involving humans were approved by the respective institutional ethics committees of the original published studies. The studies were conducted in accordance with the local legislation and institutional requirements. Written informed consent for participation was not required from the participants or the participants' legal guardians/next of kin in accordance with the national legislation and institutional requirements.

Author contributions

HX: Data curation, Visualization, Writing – original draft, Writing – review & editing. X-YL: Data curation, Writing – review & editing. H-CY: Software, Supervision, Writing – review & editing. P-LP: Conceptualization, Formal analysis, Project administration, Resources, Supervision, Writing – review & editing. S-YG: Methodology, Software, Supervision, Writing – review & editing. W-HL: Formal analysis, Resources, Supervision, Writing – review & editing. SW: Resources, Supervision, Writing – review & editing.

Funding

The author(s) declared that financial support was received for this work and/or its publication. This work was supported by the Jiangsu Commission of Health (LKZ2023019 and ZD2022009), Yancheng Commission of Health (YCBK202216), Yancheng Science and Technology Bureau (YCBK2024079 and YCBK2024018), Nantong University Special Research Fund for Clinical Medicine (2023JZ019).

Acknowledgments

We would like to thank the team of JiaJia Zhu from The First Affiliated Hospital of Anhui Medical University for providing their technical support.

Conflict of interest

The author(s) declared that this work was conducted in the absence of any commercial or financial relationships that could be construed as a potential conflict of interest.

Generative AI statement

The author(s) declared that Generative AI was used in the creation of this manuscript. During the preparation of this work, the authors used Gemini 2.5 Pro to improve the readability and language of the manuscript. After using this tool/service, the authors reviewed and edited the content as needed and take full responsibility for the content of the published article.

Any alternative text (alt text) provided alongside figures in this article has been generated by Frontiers with the support of artificial intelligence and reasonable efforts have been made to ensure accuracy, including review by the authors wherever possible. If you identify any issues, please contact us.

Publisher's note

All claims expressed in this article are solely those of the authors and do not necessarily represent those of their affiliated organizations, or those of the publisher, the editors and the reviewers. Any product that may be evaluated in this article, or claim that may be made by its manufacturer, is not guaranteed or endorsed by the publisher.

Supplementary material

The Supplementary material for this article can be found online at: <https://www.frontiersin.org/articles/10.3389/fpubh.2026.1762620/full#supplementary-material>

SUPPLEMENTARY FIGURE S1

Flow diagram of study identification and selection in accordance with PRISMA 2020 guidelines. GM, gray matter; ROI, region of interest; VBM, voxel-based morphometry.

SUPPLEMENTARY FIGURE S2

Smoking-related GM alteration networks based on 1-mm radius sphere. Smoking-related GM alteration networks are shown as network probability maps thresholded at 50%, showing brain regions functionally connected to more than 50% of the contrast seeds.

SUPPLEMENTARY FIGURE S3

Smoking-related GM alteration networks based on 7-mm radius sphere. Smoking-related GM alteration networks are shown as network probability maps thresholded at 50%, showing brain regions functionally connected to more than 50% of the contrast seeds.

SUPPLEMENTARY FIGURE S4

Associations of GM volume alteration networks with canonical brain networks in smokers based on 1-mm radius sphere. Polar plots display the proportion of overlapping voxels between each GM volume alteration network and a canonical network relative to all voxels within the corresponding canonical network. The green triangles represent GM volume alteration networks, defined as significant networks, exhibiting $\geq 10\%$ overlap with canonical networks, whereas the orange triangles represent non-significant networks with $<10\%$ overlap.

SUPPLEMENTARY FIGURE S5

Associations of GM volume alteration networks with canonical brain networks in smokers based on 7-mm radius sphere. Polar plots display the proportion of overlapping voxels between each GM volume alteration network and a canonical network relative to all voxels within the corresponding canonical network. The green triangles represent GM volume alteration networks, defined as significant networks, exhibiting $\geq 10\%$ overlap with canonical networks, whereas the orange triangles represent non-significant networks with $<10\%$ overlap.

SUPPLEMENTARY FIGURE S6

Smoking-related GM alteration networks in the higher-exposure subgroup based on a 1-mm radius sphere. Smoking-related GM alteration networks are shown as network probability maps thresholded at 60%, showing brain regions functionally connected to more than 60% of the contrast seeds.

SUPPLEMENTARY FIGURE S7

Associations of GM volume alteration networks with canonical brain networks in the higher-exposure subgroup based on a 1-mm radius sphere. Polar plots display the proportion of overlapping voxels between each GM volume alteration network and a canonical network relative to all voxels within the corresponding canonical network. The green triangles represent GM volume alteration networks, defined as significant networks, exhibiting $\geq 22\%$ overlap with canonical networks, whereas the orange triangles represent non-significant networks with $<22\%$ overlap.

SUPPLEMENTARY FIGURE S8

Smoking-related GM alteration networks in the lower-exposure subgroup based on a 1-mm radius sphere. Smoking-related GM alteration networks are shown as network probability maps thresholded at 60%, showing brain regions functionally connected to more than 60% of the contrast seeds.

SUPPLEMENTARY FIGURE S9

Associations of GM volume alteration networks with canonical brain networks in the lower-exposure subgroup based on a 1-mm radius sphere. Polar plots display the proportion of overlapping voxels between each GM volume alteration network and a canonical network relative to all voxels within the corresponding canonical network. The green triangles represent GM volume alteration networks, defined as significant networks, exhibiting $\geq 15\%$ overlap with canonical networks, whereas the orange triangles represent non-significant networks with $<15\%$ overlap.

SUPPLEMENTARY FIGURE S10

Smoking-related GM alteration networks in the higher-exposure subgroup based on a 7-mm radius sphere. Smoking-related GM alteration networks are shown as network probability maps thresholded at 60%, showing brain regions functionally connected to more than 60% of the contrast seeds.

SUPPLEMENTARY FIGURE S11

Associations of GM volume alteration networks with canonical brain networks in the higher-exposure subgroup based on a 7-mm radius sphere. Polar plots display the proportion of overlapping voxels between each GM volume alteration network and a canonical network relative to all voxels within the corresponding canonical network. The green triangles represent GM volume alteration networks, defined as significant networks, exhibiting $\geq 22\%$ overlap with canonical networks, whereas the orange triangles represent non-significant networks with $<22\%$ overlap.

SUPPLEMENTARY FIGURE S12

Smoking-related GM alteration networks in the lower-exposure subgroup based on a 7-mm radius sphere. Smoking-related GM alteration networks are shown as network probability maps thresholded at 60%, showing brain regions functionally connected to more than 60% of the contrast seeds.

SUPPLEMENTARY FIGURE S13

Associations of GM volume alteration networks with canonical brain networks in the lower-exposure subgroup based on a 7-mm radius sphere. Polar plots display the proportion of overlapping voxels between each GM volume alteration network and a canonical network relative to all voxels within the corresponding canonical network. The green triangles represent GM volume alteration networks, defined as significant networks, exhibiting $\geq 15\%$ overlap with canonical networks, whereas the orange triangles represent non-significant networks with $<15\%$ overlap.

References

- Fouad H, Commar A, Hamadeh R, El-Awa F, Shen Z, Fraser C. Estimated and projected prevalence of tobacco smoking in males, eastern Mediterranean region, 2000–2025. *East Mediterr Health J.* (2021) 27:76–82. doi: 10.26719/2021.27.1.76
- Dai X, Gil GF, Reitsma MB, Ahmad NS, Anderson JA, Bisignano C, et al. Health effects associated with smoking: a burden of proof study. *Nat Med.* (2022) 28:2045–55. doi: 10.1038/s41591-022-01978-x
- Chan KH, Wright N, Xiao D, Guo Y, Chen Y, Du H, et al. Tobacco smoking and risks of more than 470 diseases in China: a prospective cohort study. *Lancet Public Health.* (2022) 7:e1014–26. doi: 10.1016/s2468-2667(22)00227-4
- Cho ER, Brill IK, Gram IT, Brown PE, Jha P. Smoking cessation and short- and longer-term mortality. *NEJM Evid.* (2024) 3:EVIDo2300272. doi: 10.1056/EVIDo2300272
- Thomson B, Islami F. Association of Smoking Cessation and Cardiovascular, Cancer, and respiratory mortality. *JAMA Intern Med.* (2024) 184:110–2. doi: 10.1001/jamainternmed.2023.6419
- Hecht SS, Hatsukami DK. Smokeless tobacco and cigarette smoking: chemical mechanisms and cancer prevention. *Nat Rev Cancer.* (2022) 22:143–55. doi: 10.1038/s41568-021-00423-4
- Subramaniam M, Dani JA. Dopaminergic and cholinergic learning mechanisms in nicotine addiction. *Ann N Y Acad Sci.* (2015) 1349:46–63. doi: 10.1111/nyas.12871
- Wills L, Ables JL, Braunscheidel KM, Caligiuri SPB, Elayouby KS, Fillinger C, et al. Neurobiological mechanisms of nicotine reward and aversion. *Pharmacol Rev.* (2022) 74:271–310. doi: 10.1124/pharmrev.121.000299
- Piccio MR, Kenny PJ. Mechanisms of nicotine addiction. *Cold Spring Harb Perspect Med.* (2021) 11:a039610. doi: 10.1101/cshperspect.a039610
- Sharp BM, Chen H. Neurogenetic determinants and mechanisms of addiction to nicotine and smoked tobacco. *Eur J Neurosci.* (2019) 50:2164–79. doi: 10.1111/ejn.14171
- Volkow ND, Wang GJ, Fowler JS, Tomasi D, Telang F. Addiction: beyond dopamine reward circuitry. *Proc Natl Acad Sci USA.* (2011) 108:15037–42. doi: 10.1073/pnas.1010654108
- Wang Q, Du W, Wang H, Geng P, Sun Y, Zhang J, et al. Nicotine's effect on cognition, a friend or foe? *Prog Neuro-Psychopharmacol Biol Psychiatry.* (2023) 124:110723. doi: 10.1016/j.pnpbp.2023.110723
- Hajdusianek W, Żorawik A, Waliszewska-Prosół M, Poręba R, Gać P. Tobacco and nervous system development and function-new findings 2015–2020. *Brain Sci.* (2021) 11:797. doi: 10.3390/brainsci11060797
- G SB, Choi S, Krishnan J, K R. Cigarette smoke and related risk factors in neurological disorders: an update. *Biomed Pharmacother.* (2017) 85:79–86. doi: 10.1016/j.biopha.2016.11.118
- Asan L, Lalfán-Melgoza C, Beretta CA, Sack M, Zheng L, Weber-Fahr W, et al. Cellular correlates of gray matter volume changes in magnetic resonance morphometry identified by two-photon microscopy. *Sci Rep.* (2021) 11:4234. doi: 10.1038/s41598-021-83491-8
- Koster M, van der Pluijm M, Fraikin M, van Wingen G, van de Giessen E, de Haan L, et al. Tobacco smoking and Gray matter volume in individuals at clinical high risk for psychosis: a longitudinal magnetic resonance imaging study. *Biol Psychiatry Glob Open Sci.* (2025) 5:100539. doi: 10.1016/j.bpsgos.2025.100539
- Chen X, Long K, Liu S, Cai Y, Cheng L, Chen W, et al. Repeated exposure to high-dose nicotine induces prefrontal gray matter atrophy in adolescent male rats. *Neuroscience.* (2025) 566:205–17. doi: 10.1016/j.neuroscience.2024.11.059
- Seo YS, Park JM, Kim JH, Lee MY. Cigarette smoke-induced reactive oxygen species formation: a concise review. *Antioxidants.* (2023) 12:1732. doi: 10.3390/antiox12091732
- Peng P, Wang Z, Jiang T, Chu S, Wang S, Xiao D. Brain-volume changes in young and middle-aged smokers: a DARTel-based voxel-based morphometry study. *Clin Respir J.* (2017) 11:621–31. doi: 10.1111/crj.12393
- Conti AA, Baldacchino AM. Neuroanatomical correlates of impulsive choices and risky decision making in Young chronic tobacco smokers: a voxel-based morphometry study. *Front Psych.* (2021) 12:708925. doi: 10.3389/fpsy.2021.708925
- Cai Z, Wang P, Liu B, Zou Y, Wu S, Tian J, et al. To explore the mechanism of tobacco addiction using structural and functional MRI: a preliminary study of the role of the cerebellum-striatum circuit. *Brain Imaging Behav.* (2022) 16:834–42. doi: 10.1007/s11682-021-00546-0
- Bu L, Yu D, Su S, Ma Y, von Deneen KM, Luo L, et al. Functional connectivity abnormalities of brain regions with structural deficits in Young adult male smokers. *Front Hum Neurosci.* (2016) 10:494. doi: 10.3389/fnhum.2016.00494

23. Hanlon CA, Owens MM, Joseph JE, Zhu X, George MS, Brady KT, et al. Lower sub-cortical gray matter volume in both younger smokers and established smokers relative to non-smokers. *Addict Biol.* (2016) 21:185–95. doi: 10.1111/adb.12171
24. Franklin TR, Wetherill RR, Jagannathan K, Johnson B, Mumma J, Hager N, et al. The effects of chronic cigarette smoking on gray matter volume: influence of sex. *PLoS One.* (2014) 9:e104102. doi: 10.1371/journal.pone.0104102
25. Wang K, Yang J, Zhang S, Wei D, Hao X, Tu S, et al. The neural mechanisms underlying the acute effect of cigarette smoking on chronic smokers. *PLoS One.* (2014) 9:e102828. doi: 10.1371/journal.pone.0102828
26. Gallinat J, Meisenzahl E, Jacobsen LK, Kalus P, Bierbrauer J, Kienast T, et al. Smoking and structural brain deficits: a volumetric MR investigation. *Eur J Neurosci.* (2006) 24:1744–50. doi: 10.1111/j.1460-9568.2006.05050.x
27. Zhang X, Salmeron BJ, Ross TJ, Geng X, Yang Y, Stein EA. Factors underlying pre-frontal and insula structural alterations in smokers. *NeuroImage.* (2011) 54:42–8. doi: 10.1016/j.neuroimage.2010.08.008
28. Fritz HC, Wittfeld K, Schmidt CO, Domin M, Grabe HJ, Hegenscheid K, et al. Current smoking and reduced gray matter volume—a voxel-based morphometry study. *Neuropsychopharmacology.* (2014) 39:2594–600. doi: 10.1038/npp.2014.112
29. Yu R, Zhao L, Lu L. Regional grey and white matter changes in heavy male smokers. *PLoS One.* (2011) 6:e27440. doi: 10.1371/journal.pone.0027440
30. Zhang M, Gao X, Yang Z, Niu X, Wang W, Han S, et al. Integrative brain structural and molecular analyses of interaction between tobacco use disorder and overweight among male adults. *J Neurosci Res.* (2022) 101:232–44. doi: 10.1002/jnr.25141
31. Vanasse TJ, Fox PM, Barron DS, Robertson M, Eickhoff SB, Lancaster JL, et al. BrainMap VBM: an environment for structural meta-analysis. *Hum Brain Mapp.* (2018) 39:3308–25. doi: 10.1002/hbm.24078
32. Shen Z, Huang P, Wang C, Qian W, Yang Y, Zhang M. Cerebellar gray matter reductions associate with decreased functional connectivity in nicotine-dependent individuals. *Nicotine Tobacco Res.* (2018) 20:440–7. doi: 10.1093/ntr/ntx168
33. McClernon FJ, Gilbert DG. Human functional neuroimaging in nicotine and tobacco research: basics, background, and beyond. *Nicotine Tob Res.* (2004) 6:941–59. doi: 10.1080/14622200412331337394
34. Wen J, Antoniadis M, Yang Z, Hwang G, Skampardon I, Wang R, et al. Dimensional neuroimaging Endophenotypes: neurobiological representations of disease heterogeneity through machine learning. *Biol Psychiatry.* (2024) 96:564–84. doi: 10.1016/j.biopsych.2024.04.017
35. Kouri N, Frankenhauser I, Peng Z, Labuzan SA, Boon BDC, Moloney CM, et al. Clinicopathologic heterogeneity and glial activation patterns in Alzheimer disease. *JAMA Neurol.* (2024) 81:619–29. doi: 10.1001/jamaneurol.2024.0784
36. Laumann TO, Zorumski CF, Dosenbach NUF. Precision neuroimaging for localization-related psychiatry. *JAMA Psychiatry.* (2023) 80:763–4. doi: 10.1001/jamapsychiatry.2023.1576
37. Poldrack RA, Baker CI, Durnez J, Gorgolewski KJ, Matthews PM, Munafò MR, et al. Scanning the horizon: towards transparent and reproducible neuroimaging research. *Nat Rev Neurosci.* (2017) 18:115–26. doi: 10.1038/nrn.2016.167
38. Ma L, Tao Q, Dang J, Sun J, Niu X, Zhang M, et al. The structural and functional brain alterations in tobacco use disorder: a systematic review and meta-analysis. *Front Psych.* (2025) 16:1403604. doi: 10.3389/fpsy.2025.1403604
39. Pan P, Shi H, Zhong J, Xiao P, Shen Y, Wu L, et al. Chronic smoking and brain gray matter changes: evidence from meta-analysis of voxel-based morphometry studies. *Neurol Sci.* (2013) 34:813–7. doi: 10.1007/s10072-012-1256-x
40. Yang Z, Zhang Y, Cheng J, Zheng R. Meta-analysis of brain gray matter changes in chronic smokers. *Eur J Radiol.* (2020) 132:109300. doi: 10.1016/j.ejrad.2020.109300
41. Tench CR, Tanasescu R, Constantinescu CS, Cottam WJ, Auer DP. Coordinate based meta-analysis of networks in neuroimaging studies. *NeuroImage.* (2020) 205:116259. doi: 10.1016/j.neuroimage.2019.116259
42. Fornito A, Zalesky A, Breakspear M. The connectomics of brain disorders. *Nat Rev Neurosci.* (2015) 16:159–72. doi: 10.1038/nrn3901
43. Fox MD. Mapping symptoms to brain networks with the human connectome. *N Engl J Med.* (2018) 379:2237–45. doi: 10.1056/NEJMr1706158
44. Taylor JJ, Siddiqi SH, Fox MD. Coordinate network mapping: an emerging approach for morphometric Meta-analysis. *Am J Psychiatry.* (2021) 178:1080–1. doi: 10.1176/appi.ajp.2021.21100987
45. Zhang M, Sun J, Tao Q, Dang J, Wang W, Han S, et al. Abnormal resting-state effective connectivity of triple network predicts smoking motivations among males. *Front Psych.* (2025) 16:1622162. doi: 10.3389/fpsy.2025.1622162
46. Ding X, Lee SW. Changes of functional and effective connectivity in smoking replenishment on deprived heavy smokers: a resting-state fMRI study. *PLoS One.* (2013) 8:e59331. doi: 10.1371/journal.pone.0059331
47. Ely AV, Jagannathan K, Spilka N, Keyser H, Rao H, Franklin TR, et al. Exploration of the influence of body mass index on intra-network resting-state connectivity in chronic cigarette smokers. *Drug Alcohol Depend.* (2021) 227:108911. doi: 10.1016/j.drugalcdep.2021.108911
48. Tolomeo S, Yu R. Brain network dysfunctions in addiction: a meta-analysis of resting-state functional connectivity. *Transl Psychiatry.* (2022) 12:41. doi: 10.1038/s41398-022-01792-6
49. Joutsa J, Moussawi K, Siddiqi SH, Abdolahi A, Drew W, Cohen AL, et al. Brain lesions disrupting addiction map to a common human brain circuit. *Nat Med.* (2022) 28:1249–55. doi: 10.1038/s41591-022-01834-y
50. Darby RR, Joutsa J, Fox MD. Network localization of heterogeneous neuroimaging findings. *Brain.* (2019) 142:70–9. doi: 10.1093/brain/awy292
51. Peng S, Xu P, Jiang Y, Gong G. Activation network mapping for integration of heterogeneous fMRI findings. *Nat Hum Behav.* (2022) 6:1417–29. doi: 10.1038/s41562-022-01371-1
52. Taylor JJ, Lin C, Talmasov D, Ferguson MA, Schaper F, Jiang J, et al. A transdiagnostic network for psychiatric illness derived from atrophy and lesions. *Nat Hum Behav.* (2023) 7:420–9. doi: 10.1038/s41562-022-01501-9
53. Page MJ, McKenzie JE, Bossuyt PM, Boutron I, Hoffmann TC, Mulrow CD, et al. The PRISMA 2020 statement: an updated guideline for reporting systematic reviews. *BMJ.* (2021) 372:n71. doi: 10.1136/bmj.n71
54. Lancaster JL, Tordesillas-Gutiérrez D, Martínez M, Salinas F, Evans A, Zilles K, et al. Bias between MNI and Talairach coordinates analyzed using the ICBM-152 brain template. *Hum Brain Mapp.* (2007) 28:1194–205. doi: 10.1002/hbm.20345
55. Elam JS, Glasser MF, Harms MP, Sotiropoulos SN, Andersson JLR, Burgess GC, et al. The human connectome project: a retrospective. *NeuroImage.* (2021) 244:118543. doi: 10.1016/j.neuroimage.2021.118543
56. Yan CG, Wang XD, Zuo XN, Zang YF. DPABI: data processing and analysis for (resting-state) brain imaging. *Neuroinformatics.* (2016) 14:339–51. doi: 10.1007/s12021-016-9299-4
57. Murphy K, Fox MD. Towards a consensus regarding global signal regression for resting state functional connectivity MRI. *NeuroImage.* (2017) 154:169–73. doi: 10.1016/j.neuroimage.2016.11.052
58. Murphy K, Birn RM, Handwerker DA, Jones TB, Bandettini PA. The impact of global signal regression on resting state correlations: are anti-correlated networks introduced? *NeuroImage.* (2009) 44:893–905. doi: 10.1016/j.neuroimage.2008.09.036
59. Shirer WR, Ryali S, Rykhlevskaia E, Menon V, Greicius MD. Decoding subject-driven cognitive states with whole-brain connectivity patterns. *Cereb Cortex.* (2012) 22:158–65. doi: 10.1093/cercor/bhr099
60. Prillwitz CC, Rüber T, Reuter M, Montag C, Weber B, Elger CE, et al. The salience network and human personality: integrity of white matter tracts within anterior and posterior salience network relates to the self-directedness character trait. *Brain Res.* (2018) 1692:66–73. doi: 10.1016/j.brainres.2018.04.035
61. Corbetta M, Shulman GL. Control of goal-directed and stimulus-driven attention in the brain. *Nat Rev Neurosci.* (2002) 3:201–15. doi: 10.1038/nrn755
62. Rose EJ, Ross TJ, Kurup PK, Stein EA. Nicotine modulation of information processing is not limited to input (attention) but extends to output (intention). *Psychopharmacology.* (2010) 209:291–302. doi: 10.1007/s00213-010-1788-9
63. Weiland BJ, Sabbineni A, Calhoun VD, Welsh RC, Hutchison KE. Reduced executive and default network functional connectivity in cigarette smokers. *Hum Brain Mapp.* (2015) 36:872–82. doi: 10.1002/hbm.22672
64. Zhang T, Luo X, Zeng Q, Li K, Chen Y, Sun Y, et al. Smoking alters effective connectivity of resting-state brain networks in mild cognitive impairment. *J Alzheimer's Dis.* (2025) 105:893–903. doi: 10.1177/13872877251333152
65. Seeley WW, Menon V, Schatzberg AF, Keller J, Glover GH, Kenna H, et al. Dissociable intrinsic connectivity networks for salience processing and executive control. *J Neurosci.* (2007) 27:2349–56. doi: 10.1523/jneurosci.5587-06.2007
66. Holmes CJ, Barton AW, MacKillop J, Galván A, Owens MM, McCormick MJ, et al. Parenting and salience network connectivity among African Americans: a protective pathway for health-risk behaviors. *Biol Psychiatry.* (2018) 84:365–71. doi: 10.1016/j.biopsych.2018.03.003
67. Chiong W, Wilson SM, D'Esposito M, Kayser AS, Grossman SN, Poorzand P, et al. The salience network causally influences default mode network activity during moral reasoning. *Brain.* (2013) 136:1929–41. doi: 10.1093/brain/awt066
68. Chong JSX, Ng GJP, Lee SC, Zhou J. Salience network connectivity in the insula is associated with individual differences in interoceptive accuracy. *Brain Struct Funct.* (2017) 222:1635–44. doi: 10.1007/s00429-016-1297-7
69. Li Y, Yuan K, Guan Y, Cheng J, Bi Y, Shi S, et al. The implication of salience network abnormalities in young male adult smokers. *Brain Imaging Behav.* (2017) 11:943–53. doi: 10.1007/s11682-016-9568-8
70. Bi Y, Yuan K, Guan Y, Cheng J, Zhang Y, Li Y, et al. Altered resting state functional connectivity of anterior insula in young smokers. *Brain Imaging Behav.* (2017) 11:155–65. doi: 10.1007/s11682-016-9511-z
71. James AC, Pizzagalli DA, Richardt S, de Bf B, Chuzy S, Pachas G, et al. Brain reactivity to smoking cues prior to smoking cessation predicts ability to maintain tobacco abstinence. *Biol Psychiatry.* (2010) 67:722–9. doi: 10.1016/j.biopsych.2009.12.034
72. Moran LV, Sampath H, Stein EA, Hong LE. Insular and anterior cingulate circuits in smokers with schizophrenia. *Schizophr Res.* (2012) 142:223–9. doi: 10.1016/j.schres.2012.08.033
73. Zhang T, Luo X, Zeng Q, Fu Y, Li Z, Li K, et al. Effects of smoking on regional homogeneity in mild cognitive impairment: a resting-state functional MRI study. *Front Aging Neurosci.* (2020) 12:572732. doi: 10.3389/fnagi.2020.572732

74. Zhang S, Hu S, Fucito LM, Luo X, Mazure CM, Zaborszky L, et al. Resting-state functional connectivity of the basal nucleus of Meynert in cigarette smokers: dependence level and gender differences. *Nicotine Tob Res.* (2017) 19:452–9. doi: 10.1093/ntr/ntw209
75. Wu G, Yang S, Zhu L, Lin F. Altered spontaneous brain activity in heavy smokers revealed by regional homogeneity. *Psychopharmacology.* (2015) 232:2481–9. doi: 10.1007/s00213-015-3881-6
76. Cheng W, Rolls ET, Robbins TW, Gong W, Liu Z, Lv W, et al. Decreased brain connectivity in smoking contrasts with increased connectivity in drinking. *eLife.* (2019) 8:e40765. doi: 10.7554/eLife.40765
77. Durazzo TC, Meyerhoff DJ, Murray DE. Comparison of regional brain perfusion levels in chronically smoking and non-smoking adults. *Int J Environ Res Public Health.* (2015) 12:8198–213. doi: 10.3390/ijerph120708198
78. Stoeckel LE, Chai XJ, Zhang J, Whitfield-Gabrieli S, Evins AE. Lower gray matter density and functional connectivity in the anterior insula in smokers compared with never smokers. *Addict Biol.* (2016) 21:972–81. doi: 10.1111/adb.12262
79. Naqvi NH, Rudrauf D, Damasio H, Bechara A. Damage to the insula disrupts addiction to cigarette smoking. *Science.* (2007) 315:531–4. doi: 10.1126/science.1135926
80. Pan Y, Bi C, Ye Z, Lee H, Yu J, Yammine L, et al. Tobacco smoking functional networks: a whole-brain connectome analysis in 24,539 individuals. *Nicotine Tob Res.* (2024) 27:917–25. doi: 10.1093/ntr/ntae256
81. Dias NR, Peechatka AL, Janes AC. Insula reactivity to negative stimuli is associated with daily cigarette use: a preliminary investigation using the human connectome database. *Drug Alcohol Depend.* (2016) 159:277–80. doi: 10.1016/j.drugalcdep.2015.12.010
82. Zhou S, Xiao D, Peng P, Wang SK, Liu Z, Qin HY, et al. Effect of smoking on resting-state functional connectivity in smokers: an fMRI study. *Respirology.* (2017) 22:1118–24. doi: 10.1111/resp.13048
83. Faulkner P, Ghahremani DG, Tyndale RF, Paterson NE, Cox C, Ginder N, et al. Neural basis of smoking-induced relief of craving and negative affect: contribution of nicotine. *Addict Biol.* (2019) 24:1087–95. doi: 10.1111/adb.12679
84. Gunn MP, Rose GM, Whitton AE, Pizzagalli DA, Gilbert DG. Smoking progression and nicotine-enhanced reward sensitivity predicted by resting-state functional connectivity in salience and executive control networks. *Nicotine Tob Res.* (2024) 26:1305–12. doi: 10.1093/ntr/ntae084
85. Cushnie AK, Tang W, Heilbronner SR. Connecting circuits with networks in addiction neuroscience: a salience network perspective. *Int J Mol Sci.* (2023) 24:9083. doi: 10.3390/ijms24109083
86. Fedota JR, Matous AL, Salmeron BJ, Gu H, Ross TJ, Stein EA. Insula demonstrates a non-linear response to varying demand for cognitive control and weaker resting connectivity with the executive control network in smokers. *Neuropsychopharmacology.* (2016) 41:2557–65. doi: 10.1038/npp.2016.62
87. Fedota JR, Ding X, Matous AL, Salmeron BJ, McKenna MR, Gu H, et al. Nicotine abstinence influences the calculation of salience in discrete insular circuits. *Biol Psychiatry: Cognit Neurosci Neuroimaging.* (2018) 3:150–9. doi: 10.1016/j.bpsc.2017.09.010
88. Lerman C, Gu H, Loughhead J, Ruparel K, Yang Y, Stein EA. Large-scale brain network coupling predicts acute nicotine abstinence effects on craving and cognitive function. *JAMA Psychiatry.* (2014) 71:523–30. doi: 10.1001/jamapsychiatry.2013.4091
89. Abdolahi A, Williams GC, Benesch CG, Wang HZ, Spitzer EM, Scott BE, et al. Immediate and sustained decrease in smoking urges after acute insular cortex damage. *Nicotine Tob Res.* (2017) 19:756–62. doi: 10.1093/ntr/ntx046
90. Regner ME, Tregellas J, Kluger B, Wylie K, Gowin JL, Tanabe J. The insula in nicotine use disorder: functional neuroimaging and implications for neuromodulation. *Neurosci Biobehav Rev.* (2019) 103:414–24. doi: 10.1016/j.neubiorev.2019.06.002
91. Hou L, Zhang J, Liu J, Chen C, Gao X, Chen L, et al. Two-hour nicotine withdrawal improves inhibitory control dysfunction in male smokers: evidence from a smoking-cued go/no-go task ERP study. *Neuropsychiatr Dis Treat.* (2024) 20:863–75. doi: 10.2147/ndt.S452795
92. Li X, Hartwell KJ, Borckardt J, Prisciandaro JJ, Saladin ME, Morgan PS, et al. Volitional reduction of anterior cingulate cortex activity produces decreased cue craving in smoking cessation: a preliminary real-time fMRI study. *Addict Biol.* (2013) 18:739–48. doi: 10.1111/j.1369-1600.2012.00449.x
93. Azizian A, Nestor LJ, Payer D, Monterosso JR, Brody AL, London ED. Smoking reduces conflict-related anterior cingulate activity in abstinent cigarette smokers performing a Stroop task. *Neuropsychopharmacology.* (2010) 35:775–82. doi: 10.1038/npp.2009.186
94. Zanchi D, Brody AL, Montandon ML, Kopel R, Emmert K, Preti MG, et al. Cigarette smoking leads to persistent and dose-dependent alterations of brain activity and connectivity in anterior insula and anterior cingulate. *Addict Biol.* (2015) 20:1033–41. doi: 10.1111/adb.12292
95. Allenby C, Falcone M, Wileyto EP, Cao W, Bernardo L, Ashare RL, et al. Neural cue reactivity during acute abstinence predicts short-term smoking relapse. *Addict Biol.* (2020) 25:e12733. doi: 10.1111/adb.12733
96. Tang YY, Tang R, Posner MI. Brief meditation training induces smoking reduction. *Proc Natl Acad Sci USA.* (2013) 110:13971–5. doi: 10.1073/pnas.1311887110
97. Westbrook C, Creswell JD, Tabibnia G, Julson E, Kober H, Tindle HA. Mindful attention reduces neural and self-reported cue-induced craving in smokers. *Soc Cogn Affect Neurosci.* (2013) 8:73–84. doi: 10.1093/scan/nsr076
98. Padula CB, Tenekedjieva LT, McCalley DM, Al-Dasouqi H, Hanlon CA, Williams LM, et al. Targeting the salience network: a mini-review on a novel neuromodulation approach for treating alcohol use disorder. *Front Psych.* (2022) 13:893833. doi: 10.3389/fpsy.2022.893833
99. Lanciego JL, Luquin N, Obeso JA. Functional neuroanatomy of the basal ganglia. *Cold Spring Harb Perspect Med.* (2012) 2:a009621. doi: 10.1101/cshperspect.a009621
100. Macpherson T, Hikida T. Role of basal ganglia neurocircuitry in the pathology of psychiatric disorders. *Psychiatry Clin Neurosci.* (2019) 73:289–301. doi: 10.1111/pcn.12830
101. Arsalidou M, Vijayarajah S, Sharaev M. Basal ganglia lateralization in different types of reward. *Brain Imaging Behav.* (2020) 14:2618–46. doi: 10.1007/s11682-019-00215-3
102. Haber S. Parallel and integrative processing through the basal ganglia reward circuit: lessons from addiction. *Biol Psychiatry.* (2008) 64:173–4. doi: 10.1016/j.biopsych.2008.05.033
103. Martin-Soelch C. Neuroadaptive changes associated with smoking: structural and functional neural changes in nicotine dependence. *Brain Sci.* (2013) 3:159–76. doi: 10.3390/brainsci3010159
104. Li S, Zhang Z, Jiang A, Ma X, Wang M, Ni H, et al. Repetitive transcranial magnetic stimulation reshaped the dynamic reconfiguration of the executive and reward networks in individuals with tobacco use disorder. *J Affect Disord.* (2024) 365:427–36. doi: 10.1016/j.jad.2024.08.120
105. Berkman ET, Falk EB, Lieberman MD. In the trenches of real-world self-control: neural correlates of breaking the link between craving and smoking. *Psychol Sci.* (2011) 22:498–506. doi: 10.1177/0956797611400918
106. Grahm JA, Parkinson JA, Owen AM. The cognitive functions of the caudate nucleus. *Prog Neurobiol.* (2008) 86:141–55. doi: 10.1016/j.pneurobio.2008.09.004
107. Graff-Radford J, Williams L, Jones DT, Benarroch EE. Caudate nucleus as a component of networks controlling behavior. *Neurology.* (2017) 89:2192–7. doi: 10.1212/wnl.0000000000004680
108. Yuan K, Yu D, Bi Y, Li Y, Guan Y, Liu J, et al. The implication of frontostriatal circuits in young smokers: a resting-state study. *Hum Brain Mapp.* (2016) 37:2013–26. doi: 10.1002/hbm.23153
109. Zubietta JK, Heitzeg MM, Xu Y, Koeppe RA, Ni L, Guthrie S, et al. Regional cerebral blood flow responses to smoking in tobacco smokers after overnight abstinence. *Am J Psychiatry.* (2005) 162:567–77. doi: 10.1176/appi.ajp.162.3.567
110. Akkermans SEA, Luijten M, van Rooij D, Franken IHA, Buitelaar JK. Putamen functional connectivity during inhibitory control in smokers and non-smokers. *Addict Biol.* (2018) 23:359–68. doi: 10.1111/adb.12482
111. Brody AL, Olmstead RE, London ED, Farahi J, Meyer JH, Grossman P, et al. Smoking-induced ventral striatum dopamine release. *Am J Psychiatry.* (2004) 161:1211–8. doi: 10.1176/appi.ajp.161.7.1211
112. Salokangas RK, Vilkinen H, Ilonen T, Taiminen T, Bergman J, Haaparanta M, et al. High levels of dopamine activity in the basal ganglia of cigarette smokers. *Am J Psychiatry.* (2000) 157:632–4. doi: 10.1176/appi.ajp.157.4.632
113. Gaznick N, Tranel D, McNutt A, Bechara A. Basal ganglia plus insula damage yields stronger disruption of smoking addiction than basal ganglia damage alone. *Nicotine Tob Res.* (2014) 16:445–53. doi: 10.1093/ntr/ntt172
114. Vannemreddy P, Slavin K. Nucleus accumbens as a novel target for deep brain stimulation in the treatment of addiction: a hypothesis on the neurochemical and morphological basis. *Neuro India.* (2019) 67:1220–4. doi: 10.4103/0028-3886.271239
115. Pelloux Y, Degoulet M, Tiran-Cappello A, Cohen C, Lardeux S, George O, et al. Subthalamic nucleus high frequency stimulation prevents and reverses escalated cocaine use. *Mol Psychiatry.* (2018) 23:2266–76. doi: 10.1038/s41380-018-0080-y
116. Carpenter MJ, Saladin ME, Larowe SD, McClure EA, Simonian S, Upadhyaya HP, et al. Craving, cue reactivity, and stimulus control among early-stage young smokers: effects of smoking intensity and gender. *Nicotine Tob Res.* (2014) 16:208–15. doi: 10.1093/ntr/ntt147
117. Motschman CA, Tiffany ST. Combined smoking and alcohol cues: effects on craving, drug-seeking, and consumption. *Alcohol Clin Exp Res.* (2021) 45:1864–76. doi: 10.1111/acer.14662
118. Wei YC, Kung YC, Huang WY, Lin C, Chen YL, Chen CK, et al. Functional connectivity dynamics altered of the resting brain in subjective cognitive decline. *Front Aging Neurosci.* (2022) 14:817137. doi: 10.3389/fnagi.2022.817137
119. Kuiper JJ, Lin YH, Young IM, Bai MY, Briggs RG, Tanglay O, et al. A parcellation-based model of the auditory network. *Hear Res.* (2020) 396:108078. doi: 10.1016/j.heares.2020.108078
120. Dawes P, Cruickshanks KJ, Moore DR, Edmondson-Jones M, McCormack A, Fortnum H, et al. Cigarette smoking, passive smoking, alcohol consumption, and hearing loss. *J Assoc Res Otolaryngol.* (2014) 15:663–74. doi: 10.1007/s10162-014-0461-0
121. Chang J, Ryou N, Jun HJ, Hwang SY, Song JJ, Chae SW. Effect of cigarette smoking and passive smoking on hearing impairment: data from a population-based study. *PLoS One.* (2016) 11:e0146608. doi: 10.1371/journal.pone.0146608
122. Lin BM, Wang M, Stankovic KM, Eavey R, McKenna MJ, Curhan GC, et al. Cigarette smoking, smoking cessation, and risk of hearing loss in women. *Am J Med.* (2020) 133:1180–6. doi: 10.1016/j.amjmed.2020.03.049

123. Wang C, Shen Z, Huang P, Qian W, Yu X, Sun J, et al. Altered spontaneous activity of posterior cingulate cortex and superior temporal gyrus are associated with a smoking cessation treatment outcome using varenicline revealed by regional homogeneity. *Brain Imaging Behav.* (2017) 11:611–8. doi: 10.1007/s11682-016-9538-1
124. Weng JC, Huang SY, Lee MS, Ho MC. Association between functional brain alterations and neuropsychological scales in male chronic smokers using resting-state fMRI. *Psychopharmacology.* (2021) 238:1387–99. doi: 10.1007/s00213-021-05819-6
125. Howard MA, Volkov IO, Mirsky R, Garell PC, Noh MD, Granner M, et al. Auditory cortex on the human posterior superior temporal gyrus. *J Comp Neurol.* (2000) 416:79–92. doi: 10.1002/(sici)1096-9861(20000103)416:1<79::aid-cne6>3.0.co;2-2
126. Bueti D, van Dongen EV, Walsh V. The role of superior temporal cortex in auditory timing. *PLoS One.* (2008) 3:e2481. doi: 10.1371/journal.pone.0002481
127. Ding H, Ming D, Wan B, Li Q, Qin W, Yu C. Enhanced spontaneous functional connectivity of the superior temporal gyrus in early deafness. *Sci Rep.* (2016) 6:23239. doi: 10.1038/srep23239
128. Tregellas JR, Shatti S, Tanabe JL, Martin LE, Gibson L, Wylie K, et al. Gray matter volume differences and the effects of smoking on gray matter in schizophrenia. *Schizophr Res.* (2007) 97:242–9. doi: 10.1016/j.schres.2007.08.019
129. Durazzo TC, Mon A, Pennington D, Abé C, Gazdzinski S, Meyerhoff DJ. Interactive effects of chronic cigarette smoking and age on brain volumes in controls and alcohol-dependent individuals in early abstinence. *Addict Biol.* (2014) 19:132–43. doi: 10.1111/j.1369-1600.2012.00492.x
130. Karama S, Ducharme S, Corley J, Chouinard-Decorte F, Starr JM, Wardlaw JM, et al. Cigarette smoking and thinning of the brain's cortex. *Mol Psychiatry.* (2015) 20:778–85. doi: 10.1038/mp.2014.187
131. Kushnir V, Menon M, Balducci XL, Selby P, Busto I, Zawertailo L. Enhanced smoking cue salience associated with depression severity in nicotine-dependent individuals: a preliminary fMRI study. *Int J Neuropsychopharmacol.* (2013) 16:997–1008. doi: 10.1017/s1461145710000696
132. Lee JH, Lim Y, Wiederhold BK, Graham SJ. A functional magnetic resonance imaging (fMRI) study of cue-induced smoking craving in virtual environments. *Appl Psychophysiol Biofeedback.* (2005) 30:195–204. doi: 10.1007/s10484-005-6377-z
133. Dinh-Williams L, Mendrek A, Bourque J, Potvin S. Where there's smoke, there's fire: the brain reactivity of chronic smokers when exposed to the negative value of smoking. *Prog Neuro-Psychopharmacol Biol Psychiatry.* (2014) 50:66–73. doi: 10.1016/j.pnpbp.2013.12.009
134. Buckner RL, Andrews-Hanna JR, Schacter DL. The brain's default network: anatomy, function, and relevance to disease. *Ann N Y Acad Sci.* (2008) 1124:1–38. doi: 10.1196/annals.1440.011
135. Zhang M, Dang J, Sun J, Tao Q, Niu X, Wang W, et al. Effective connectivity of default mode network subsystems and automatic smoking behaviour among males. *J Psychiatry Neurosci.* (2024) 49:E429–39. doi: 10.1503/jpn.240058
136. Ward HB, Beermann A, Nawaz U, Halko MA, Janes AC, Moran LV, et al. Evidence for schizophrenia-specific pathophysiology of nicotine dependence. *Front Psych.* (2022) 13:804055. doi: 10.3389/fpsy.2022.804055
137. Durazzo TC, Meyerhoff DJ, Yoder KK. Cigarette smoking is associated with cortical thinning in anterior frontal regions, insula and regions showing atrophy in early Alzheimer's disease. *Drug Alcohol Depend.* (2018) 192:277–84. doi: 10.1016/j.drugalcdep.2018.08.009
138. Alain C, He Y, Grady C. The contribution of the inferior parietal lobe to auditory spatial working memory. *J Cogn Neurosci.* (2008) 20:285–95. doi: 10.1162/jocn.2008.20014
139. Numssen O, Bzdok D, Hartwigsen G. Functional specialization within the inferior parietal lobes across cognitive domains. *eLife.* (2021) 10:e63591. doi: 10.7554/eLife.63591
140. Durazzo TC, Insel PS, Weiner MW. Greater regional brain atrophy rate in healthy elderly subjects with a history of cigarette smoking. *Alzheimers Dement.* (2012) 8:513–9. doi: 10.1016/j.jalz.2011.10.006
141. Zhang T, Zeng Q, Li K, Liu X, Fu Y, Qiu T, et al. Distinct resting-state functional connectivity patterns of anterior insula affected by smoking in mild cognitive impairment. *Brain Imaging Behav.* (2023) 17:386–94. doi: 10.1007/s11682-023-00766-6
142. Zhang M, Huang H, Niu X, Dang J, Sun J, Tao Q, et al. Altered inter-hemispheric and intra-hemispheric functional connectivity dynamics in male cigarette smokers. *BMC Psychiatry.* (2025) 25:758. doi: 10.1186/s12888-025-07222-3
143. Machulska A, Eiler TJ, Kleinke K, Grünewald A, Brück R, Jahn K, et al. Approach bias retraining through virtual reality in smokers willing to quit smoking: a randomized-controlled study. *Behav Res Ther.* (2021) 141:103858. doi: 10.1016/j.brat.2021.103858
144. Qiu T, Xie F, Zeng Q, Shen Z, Du G, Xu X, et al. Interactions between cigarette smoking and cognitive status on functional connectivity of the cortico-striatal circuits in individuals without dementia: a resting-state functional MRI study. *CNS Neurosci Ther.* (2022) 28:1195–204. doi: 10.1111/cns.13852
145. Tang R, Razi A, Friston KJ, Tang YY. Mapping smoking addiction using effective connectivity analysis. *Front Hum Neurosci.* (2016) 10:195. doi: 10.3389/fnhum.2016.00195
146. Naqvi NH, Bechara A. The hidden island of addiction: the insula. *Trends Neurosci.* (2009) 32:56–67. doi: 10.1016/j.tins.2008.09.009
147. Zhang R, Volkow ND. Brain default-mode network dysfunction in addiction. *NeuroImage.* (2019) 200:313–31. doi: 10.1016/j.neuroimage.2019.06.036
148. Fedota JR, Stein EA. Resting-state functional connectivity and nicotine addiction: prospects for biomarker development. *Ann N Y Acad Sci.* (2015) 1349:64–82. doi: 10.1111/nyas.12882
149. Croce P, Zappasodi F, Capotosto P. Offline stimulation of human parietal cortex differently affects resting EEG microstates. *Sci Rep.* (2018) 8:1287. doi: 10.1038/s41598-018-19698-z
150. Zhang J, Raya J, Morfini F, Urban Z, Pagliaccio D, Yendiki A, et al. Reducing default mode network connectivity with mindfulness-based fMRI neurofeedback: a pilot study among adolescents with affective disorder history. *Mol Psychiatry.* (2023) 28:2540–8. doi: 10.1038/s41380-023-02032-z
151. Fahmy R, Wasfi M, Mamdouh R, Moussa K, Wahba A, Schmitgen MM, et al. Mindfulness-based therapy modulates default-mode network connectivity in patients with opioid dependence. *Eur Neuropsychopharmacol.* (2019) 29:662–71. doi: 10.1016/j.euroneuro.2019.03.002
152. Wang Y, Yang Y, Xu W, Yao X, Xie X, Zhang L, et al. Heterogeneous brain abnormalities in schizophrenia converge on a common network associated with symptom remission. *Schizophr Bull.* (2024) 50:545–56. doi: 10.1093/schbul/sbae003
153. Cheng Y, Cai H, Liu S, Yang Y, Pan S, Zhang Y, et al. Brain network localization of Gray matter atrophy and neurocognitive and social cognitive dysfunction in schizophrenia. *Biol Psychiatry.* (2025) 97:148–56. doi: 10.1016/j.biopsych.2024.07.021
154. Kozak K, Lucatch AM, Lowe DJE, Balodis IM, MacKillop J, George TP. The neurobiology of impulsivity and substance use disorders: implications for treatment. *Ann N Y Acad Sci.* (2019) 1451:71–91. doi: 10.1111/nyas.13977
155. Zhang M, Gao X, Yang Z, Wen M, Huang H, Zheng R, et al. Shared gray matter alterations in subtypes of addiction: a voxel-wise meta-analysis. *Psychopharmacology.* (2021) 238:2365–79. doi: 10.1007/s00213-021-05920-w
156. Xu R, Zhang X, Zhou S, Guo L, Mo F, Ma H, et al. Brain structural damage networks at different stages of schizophrenia. *Psychol Med.* (2024) 54:4809–19. doi: 10.1017/s0033291724003088
157. Boes AD, Prasad S, Liu H, Liu Q, Pascual-Leone A, Caviness VS Jr, et al. Network localization of neurological symptoms from focal brain lesions. *Brain.* (2015) 138:3061–75. doi: 10.1093/brain/awv228
158. Fox MD, Buckner RL, Liu H, Chakravarty MM, Lozano AM, Pascual-Leone A. Resting-state networks link invasive and noninvasive brain stimulation across diverse psychiatric and neurological diseases. *Proc Natl Acad Sci USA.* (2014) 111:E4367–75. doi: 10.1073/pnas.1405003111
159. Horn A, Reich M, Vorwerk J, Li N, Wenzel G, Fang Q, et al. Connectivity predicts deep brain stimulation outcome in Parkinson disease. *Ann Neurol.* (2017) 82:67–78. doi: 10.1002/ana.24974
160. Burke MJ, Jouts J, Cohen AL, Soussand L, Cooke D, Burstein R, et al. Mapping migraine to a common brain network. *Brain.* (2020) 143:541–53. doi: 10.1093/brain/awz405
161. Meysami S, Garg S, Hashemi S, Akbari N, Gouda A, Chodakiewicz YG, et al. Smoking predicts brain atrophy in 10,134 healthy individuals and is potentially influenced by body mass index. *NPJ Dement.* (2025) 1:17. doi: 10.1038/s44400-025-00024-0
162. Durazzo TC, Meyerhoff DJ, Nixon SJ. Chronic cigarette smoking: implications for neurocognition and brain neurobiology. *Int J Environ Res Public Health.* (2010) 7:3760–91. doi: 10.3390/ijerph7103760
163. Linli Z, Rolls ET, Zhao W, Kang J, Feng J, Guo S. Smoking is associated with lower brain volume and cognitive differences: a large population analysis based on the UK biobank. *Prog Neuro-Psychopharmacol Biol Psychiatry.* (2023) 123:110698. doi: 10.1016/j.pnpbp.2022.110698
164. Almeida OP, Garrido GJ, Alfonso H, Hulse G, Lautenschlager NT, Hankey GJ, et al. 24-month effect of smoking cessation on cognitive function and brain structure in later life. *NeuroImage.* (2011) 55:1480–9. doi: 10.1016/j.neuroimage.2011.01.063
165. Boparai K, Lin H-Y, Selby P, Zawertailo L. Grey matter morphometry in young adult e-cigarette users, tobacco cigarette users and non-using controls. *Neuropsychopharmacology.* (2025) 50:1455–63. doi: 10.1038/s41386-025-02086-3
166. Chen Y, Chaudhary S, Wang W, Li CR. Gray matter volumes of the insula and anterior cingulate cortex and their dysfunctional roles in cigarette smoking. *Addict Neurosci.* (2022) 1:100003. doi: 10.1016/j.addicn.2021.100003
167. Daniju Y, Faulkner P, Brandt K, Allen P. Prefrontal cortex and putamen grey matter alterations in cannabis and tobacco users. *J Psychopharmacol.* (2022) 36:1315–23. doi: 10.1177/02698811221117523
168. Faulkner P, Lucini Paioni S, Kozuharova P, Orlov N, Lythgoe DJ, Daniju Y, et al. Daily and intermittent smoking are associated with low prefrontal volume and low concentrations of prefrontal glutamate, creatine, myo-inositol, and N-acetylaspartate. *Addict Biol.* (2021) 26:e12986. doi: 10.1111/adb.12986
169. Kunas SL, Hilbert K, Yang Y, Richter J, Hamm A, Wittmann A, et al. The modulating impact of cigarette smoking on brain structure in panic disorder: a voxel-based morphometry study. *Soc Cogn Affect Neurosci.* (2020) 15:849–59. doi: 10.1093/scan/nsaa103
170. Liao Y, Tang J, Liu T, Chen X, Hao W. Differences between smokers and non-smokers in regional gray matter volumes: a voxel-based morphometry study. *Addict Biol.* (2010) 17:977–80. doi: 10.1111/j.1369-1600.2010.02250.x
171. Morales AM, Lee B, Hellemann G, O'Neill J, London ED. Gray-matter volume in methamphetamine dependence: cigarette smoking and changes with abstinence from methamphetamine. *Drug Alcohol Depend.* (2012) 125:230–8. doi: 10.1016/j.drugalcdep.2012.02.017

172. Qian W, Huang P, Shen Z, Wang C, Yang Y, Zhang M. Brain Gray matter volume and functional connectivity are associated with smoking cessation outcomes. *Front Hum Neurosci.* (2019) 13:361. doi: 10.3389/fnhum.2019.00361
173. Weidler C, Gramegna C, Müller D, Schrickel M, Habel U. Resting-state functional connectivity and structural differences between smokers and healthy non-smokers. *Sci Rep.* (2024) 14:6878. doi: 10.1038/s41598-024-57510-3
174. Weng JC, Chuang YC, Zheng LB, Lee MS, Ho MC. Assessment of brain connectome alterations in male chronic smokers using structural and generalized q-sampling MRI. *Brain Imaging Behav.* (2022) 16:1761–75. doi: 10.1007/s11682-022-00647-4
175. Ye Y, Zhang J, Huang B, Cai X, Wang P, Zeng P, et al. Characterizing the structural pattern of heavy smokers using multivoxel pattern analysis. *Frontiers. Psychiatry.* (2021) 11:607003. doi: 10.3389/fpsyt.2020.607003

Glossary

ACC - anterior cingulate cortex

AI - artificial intelligence

aSN - anterior Salience Network

CI - confidence interval

CS - chronic smokers

dDMN - dorsal Default Mode Network

DMN - Default Mode Network;

DPABI - data processing & analysis for brain imaging

F - female

FA, flip angle

FC - functional connectivity

FCNM - functional connectivity network mapping

FD - framewise displacement

fMRI - functional Magnetic Resonance Imaging

FOV - field of view

FSL - functional magnetic resonance imaging of the brain software library

FTND - Fagerstrom test of nicotine dependence

GM - gray matter

GRE-EPI - gradient-recalled echo-Planar Imaging

HCP - Human Connectome Project

IPL - Inferior Parietal Lobule

LECN - left executive control network

M - male

MNI - Montreal Neurological Institute

MRI - Magnetic Resonance Imaging

ms - millisecond

Na - not available

NS - non-smokers

p - *p*-value

PET - positron emission tomography

PFC - prefrontal cortex

PRISMA - Preferred Reporting Items for Systematic Reviews and Meta-Analyses

pSN - posterior Salience Network

RECEN - right executive control network

ROI - region of interest

rs-fMRI - resting-state functional Magnetic Resonance Imaging

SN - Salience Network

SD, standard deviation

SDM - seed-based d mapping

SMG - supramarginal gyrus

SPM - Statistical Parametric Mapping

STG - superior temporal gyrus

TE - echo time

TR - repetition time

VBM - voxel-based morphometry

vDMN - ventral default mode network

z - *z*-score

° - degrees